Evolution of viral quasispecies during SARS-CoV-2 infection

Aude Jary, Valentin Leducq, Isabelle Malet, Stéphane Marot, Elise Klement-Frutos, Elisa Teyssou, Cathia Soulié, Basma Abdi, Marc Wirden, Valérie Pourcher, et al.

Research Note

Title: Evolution of viral quasispecies during SARS-CoV-2 infection

A Jary[1], V. Leducq[1], I. Malet[1], S. Marot[1], E. Klement-Frutos[2], E. Teyssou[1], C. Soulié[1], B. Abdi[1], M. Wirden[1], V. Pourcher[2], E. Caumes[2], V. Calvez[1], S. Burrel[1], A-G. Marcelin[1], D. Boutolleau[1]

[1]Sorbonne Université, INSERM, Institut Pierre Louis d'Epidémiologie et de Santé Publique (iPLESP), AP-HP, Hôpital Pitié Salpêtrière, Service de Virologie, Paris, France

[2]Sorbonne Université, INSERM, Institut Pierre Louis d'Epidémiologie et de Santé Publique (iPLESP), AP-HP, Hôpital Pitié Salpêtrière, Service de Maladie Infectieuses et Tropicales, Paris, France

Corresponding author: Aude Jary, 47-83 boulevard de l'hôpital, 75013 Paris, +33142177406, aude.jary@aphp.fr

ABSTRACT

Objectives: Studies are needed to better understand the genomic evolution of the recently emerged severe acute respiratory syndrome coronavirus 2 (SARS-CoV-2). This study aimed to describe genomic diversity of SARS-CoV-2 by next generation sequencing (NGS) in a patient with longitudinal follow-up for SARS-CoV-2 infection.

Methods: Sequential samples collected from January, 29th to February, 4th, 2020 in a patient infected by SARS-CoV-2 were used to perform amplification of two genome fragments including genes encoding Spike, Envelope, Membrane and Nucleocapsid proteins, and NGS with Illumina® technology. Phylogenetic analysis was performed with PhyML and viral variant identification with VarScan.

Results: Majority consensus sequences were identical in most of the samples (5/7) and differed with one synonymous mutation from the Wuhan reference sequence. We identified 233 variants; each sample harbored in median 38 different minority variants and only 4 were shared by different samples. The frequency of mutation was similar between genes and correlated to the gene length (r=0.93, *p=0.0002).* Most of mutations were substitution variations (n=217, 93.1%) and about 50% had moderate or high impact on gene expression. Viral variants also differed between lower and upper respiratory tract samples collected on the same day, suggesting independent sites of replication of SARS-CoV-2.

Conclusion: We reported for the first time minority viral population representing up to 1% during the course of SARS-CoV-2 infection. Quasispecies were different from one day to the next, as well as between anatomical sites, suggesting that this new coronavirus appears as a complex and dynamic distributions of variants *in vivo*.

Keywords: SARS-CoV-2; quasispecies; minority variants; NGS; infection follow-up

INTRODUCTION

The severe acute respiratory syndrome coronavirus 2 (SARS-CoV-2) genome organization is similar to the other betacoronaviruses with the open reading frame (ORF) 1a/b encoding nonstructural proteins at the 5'-end, and structural proteins as follows: Spike (S)– Envelope (E)- Membrane (M)- Nucleocapsid (NC)– 3'-end[1]. Since the spike surface glycoprotein plays a major role in host cell infection, genomic variations may impact the interaction with the host receptor but also viral pathogenesis, transmissibility or infectivity [2].

As intrahost variant in a transversal study or from a same patient by Nanopore sequencing have already been reported [3,4], this study aimed to describe genomic diversity of SARS-CoV-2 by next generation sequencing (NGS) in a patient with longitudinal follow-up for SARS-CoV-2 infection.

METHODS

The first patient diagnosed with SARS-CoV-2 infection in Pitié-Salpêtrière Hospital, Paris, France, was followed daily for SARS-CoV-2 RT-PCR in respiratory samples : viral genome could be detected from January, 29th to February, 10th, 2020[5]. This patient, hospitalized at day 2 of a mild form of coronavirus disease 2019, did not receive any antiviral or immunomodulation treatment during the entire study period.

Two fragments of about 4000 nucleotide (nt) were amplified by nested PCR (Supplementary Table 1) and NGS was performed with pair-end reads (MiSeq v3, 2x300bp) on MiSeq Illumina® system. Reads were trimmed using Trimmomatic, then mapped on SARS-CoV-2 reference sequence (NC_045512.2) with Geneious Prime software and finally assembled *de novo* with Spades3.12.0[6] to generate majority consensus sequences.

Multiple alignment was performed with Mafft7 [7] and phylogenetic analysis of S, E, M and NC genes with PhyML3.0[8] and GTR substitution model with 1000 bootstraps resampling.

Intra-host variants were called using VarScan [9] with the following requirements: sequencing depth≥1,000, minor allele frequency≥1% and at least found 100 times. Intra-sample viral variants were studied by comparing each consensus sequence with all cleaned reads generated from the same sample and viral variants during follow-up by comparing consensus sequence of the first nasopharyngeal sample (01292020_NP) with all reads generated from the different samples. Synonymous mutations were identified as low impact, missense mutations and insertions with conservative inframe as moderate impact, and acquisition or loss of STOP codon as well as frameshift as high impact on gene expression.

Spearman rank correlation test was performed on GraphPad.

RESULTS

The sequencing was effective for the 7 first samples (1 induced sputum and 6 nasopharyngeal swabs) from January, 29th to February, 4th, 2020 with a Ct value of SARS-CoV-2 RT-PCR below 30. A full length fragment of 8,257 nt was generated with a median [IQR] of 45,523 [41,014-46,023] depth sequencing per sample (Supplementary Table 2).

Phylogenetic analysis

Compared to NC_045512.2 reference sequence, our majority consensus sequences differed in the S gene with only 4 variations. They all harbored the synonymous mutation 3591T>C whereas a non-synonymous mutation (859G>A) was found only in sample

02012020_NP. In sample 01312020_NP, a deletion of one nucleotide led to the appearance of a STOP codon prematurely and a non-synonymous substitution at position 3554.

By phylogenetic analysis of the 4 structural genes, our sequences clustered with all the SARS-CoV-2 reference sequences issued from NCBI database and were separated from the others human coronaviruses (Supplementary Figure 1).

Intra-sample viral variant diversity

We identified 233 viral variants and the number of variants per sample was not correlated with the depth sequencing (r=0.23 *p=0.28*).

Each sample harbored in median 38 [11-51.5] minority variants (<20%). Only 4/233 identical minority variants were common between 2 specimens and 6/233 other mutations were identified at a same position in 2 samples but induced different variants (Supplementary table 3). Although majority consensus sequences of the 2 specimens collected on January, 29th were strictly identical, each one harbored their specific viral population with 59 variants identified in the induced sputum and 40 in the nasopharyngeal specimens (Figure 1).

Nucleotide variations occurred in decreasing order in the S gene, the N gene, the ORF3a, the M gene, the ORF7a, the E gene, the ORF6, the ORF7b and the ORF8, and finally the ORF10 (Figure 2A). However according to gene length, the frequency of mutation was similar and correlated to the gene length (r=0.93, *p=0.0002*) (Figure 2B).

Most of mutations were substitution variations (217/233), including 87/233 synonymous mutations and 107/233 missense mutations. According to gene expression, 88/233 variants had a low impact, 111/233 an intermediate impact, and 23/233 a high impact (Figure 1). Between samples, only the frequency of frameshift and STOP codon was significantly and strongly correlated with the viral load (r=0.92, *p=0.0095*)(Figure 2D).

Follow-up of viral variant diversity

By comparing with the consensus sequence collected on January, 29th in nasopharyngeal site, we found the same viral quasispecies in each sample as reported above. However, three majority variants emerged in the S gene obtained from the nasopharyngeal samples collected on January, 31th and February, 1st and corresponding to the 3 mutations described previously in the consensus sequences. None of them were found in the previous and following samples as majority or minority variant (Supplementary Table 4).

DISCUSSION

The virus identified in this patient was almost identical to the reference sequence from Wuhan [1]. This result was expected as the patient was a general practitioner presumably infected by tourists from Wuhan and their guide who was later diagnosed SARS-CoV-2 positive[5].

Quasispecies in RNA viruses have been previously reported for SARS-CoV and MERS-CoV [10,11], as well as within individuals during SARS-CoV2 infection[3,12]. The present study, allowing the analysis of SARS-CoV-2 minority variants at 1%, supports the previous finding. Indeed, we found a median of 38 different viral variants per sample during the follow-up of a single patient, with almost no common variant from one day to the next one. More than half of the variants had an intermediate or high impact on gene expression and may explain the lack of persistence during time. Among the different types of mutations, the number of mutations inducing frameshift and STOP codon were highly correlated with the viral load, reflecting the loss of fitness in variants harboring deleterious mutations during intensive viral replication [13]. Otherwise, viral variant population was also different between samples from lower (induced sputum) and upper (nasopharyngeal swab) respiratory tracts collected on the

same day, suggesting independent replication process of SARS-CoV-2, as previously reported [14].

Contrary to a previous study which identified hotspot in the ORF8[15], the mutations identified in this study appeared to be spread fairly evenly throughout the sequenced fragment. Indeed, a limited number of viral variants were shared by 2 samples, the remainders (97%) being specific of each sample and occurring in different genomic sites and a strong correlation was found between the number of variant and the length of each gene.

The main limitation is that only a fragment of about 8000 nt was studied, in only one patient and during a short period of follow-up because of low viral load in samples collected after February, 5th. However, our results highlighted that during the first week of infection, the majority viral population remained identical (5/7), with several specific minority variants which did not seem to persist over time. Larger studies are needed to explore the entire intra-patient variability during the course of the infection, and in different clinical form, to better understand the impact of the minority viral population on SARS-CoV-2 evolution, physiopathology and transmission.

Acknowledgements. We thank the SMIT PSL COVID cohort Team for its support.

Funding. This study was funded by the *Agence Nationale de Recherche sur le SIDA et les Hépatites Virale*s (ANRS, AC43), the *Agence National de la Recherche* (ANR) *and Sorbonne Université.*

Author contributions. DB, AGM, SB, VC planned the research; EKF, VP and EC collected the clinical data; VL, IM, ET and CS performed the experiments; AJ, VL, BA and MW analyzed the data; AJ, SM, SB and DB wrote the paper. All the authors red and corrected the manuscript and approved the final version.

Competing interest. All the authors declare no competing interests.

Ethics: The study was carried out in accordance with the Declaration of Helsinki. It was a retrospective non-interventional study with no addition to standard care procedures. Reclassification of biological remnants into research material after completion of the ordered virological tests was approved by the local interventional review board of Pitié-Salpêtrière hospital. According to the French Public Health Code (CSP Article L.1121-1.1) such protocols are exempted from individual informed consent.

REFERENCES

[1] Chan JF-W, Kok K-H, Zhu Z, Chu H, To KK-W, Yuan S, et al. Genomic characterization of the 2019 novel human-pathogenic coronavirus isolated from a patient with atypical pneumonia after visiting Wuhan. Emerg Microbes Infect 2020;9:221–36. https://doi.org/10.1080/22221751.2020.1719902.

[2] Fung TS, Liu DX. Human Coronavirus: Host-Pathogen Interaction. Annu Rev Microbiol 2019;73:529–57. https://doi.org/10.1146/annurev-micro-020518-115759.

[3] Shen Z, Xiao Y, Kang L, Ma W, Shi L, Zhang L, et al. Genomic diversity of SARS-CoV-2 in Coronavirus Disease 2019 patients. Clin Infect Dis Off Publ Infect Dis Soc Am 2020. https://doi.org/10.1093/cid/ciaa203.

[4] To KK-W, Tsang OT-Y, Leung W-S, Tam AR, Wu T-C, Lung DC, et al. Temporal profiles of viral load in posterior oropharyngeal saliva samples and serum antibody responses during infection by SARS-CoV-2: an observational cohort study. Lancet Infect Dis 2020;20:565–74. https://doi.org/10.1016/S1473-3099(20)30196-1.

[5] Klement E, Godefroy N, Burrel S, Kornblum D, Monsel G, Bleibtreu A, et al. The first locally acquired novel case of 2019-nCoV infection in a healthcare worker in the Paris area. Clin Infect Dis Off Publ Infect Dis Soc Am 2020. https://doi.org/10.1093/cid/ciaa171.

[6] Bankevich A, Nurk S, Antipov D, Gurevich AA, Dvorkin M, Kulikov AS, et al. SPAdes: A New Genome Assembly Algorithm and Its Applications to Single-Cell Sequencing. J Comput Biol 2012;19:455–77. https://doi.org/10.1089/cmb.2012.0021.

[7] Katoh K, Standley DM. MAFFT multiple sequence alignment software version 7: improvements in performance and usability. Mol Biol Evol 2013;30:772–80. https://doi.org/10.1093/molbev/mst010.

[8] Guindon S, Dufayard J-F, Lefort V, Anisimova M, Hordijk W, Gascuel O. New algorithms and methods to estimate maximum-likelihood phylogenies: assessing the performance of PhyML 3.0. Syst Biol 2010;59:307–21. https://doi.org/10.1093/sysbio/syq010.

[9] Koboldt DC, Zhang Q, Larson DE, Shen D, McLellan MD, Lin L, et al. VarScan 2: somatic mutation and copy number alteration discovery in cancer by exome sequencing. Genome Res 2012;22:568–76. https://doi.org/10.1101/gr.129684.111.

[10] Xu D, Zhang Z, Wang F-S. SARS-associated coronavirus quasispecies in individual patients. N Engl J Med 2004;350:1366–7. https://doi.org/10.1056/NEJMc032421.

[11] Park D, Huh HJ, Kim YJ, Son D-S, Jeon H-J, Im E-H, et al. Analysis of intrapatient heterogeneity uncovers the microevolution of Middle East respiratory syndrome coronavirus. Cold Spring Harb Mol Case Stud 2016;2:a001214. https://doi.org/10.1101/mcs.a001214.

[12] Capobianchi MR, Rueca M, Messina F, Giombini E, Carletti F, Colavita F, et al. Molecular characterization of SARS-CoV-2 from the first case of COVID-19 in Italy. Clin Microbiol Infect Off Publ Eur Soc Clin Microbiol Infect Dis 2020. https://doi.org/10.1016/j.cmi.2020.03.025.

[13] Domingo E, Holland JJ. RNA virus mutations and fitness for survival. Annu Rev Microbiol 1997;51:151–78. https://doi.org/10.1146/annurev.micro.51.1.151.

[14] Wölfel R, Corman VM, Guggemos W, Seilmaier M, Zange S, Müller MA, et al. Virological assessment of hospitalized patients with COVID-2019. Nature 2020. https://doi.org/10.1038/s41586-020-2196-x.

[15] Ceraolo C, Giorgi FM. Genomic variance of the 2019-nCoV coronavirus. J Med Virol 2020;92:522–8. https://doi.org/10.1002/jmv.25700.

Figure 1: The severe acute respiratory syndrome coronavirus genome diversity during infection. A. Genome coverage (y-axis) according to nucleotide position (x-axis). **B.** Distribution (x-axis) and frequency (y-axis) of the 233 intra-sample viral variants identified. *Each sample is represented by the same color in figure 1A and 1B and the impact of mutations on gene expression by different symbol (low: a rhombus, moderate: a square, high: a circle).*

Figure 2: Distribution of mutation frequency and correlation with the gene length or the viral load. A: HeatMap representing the frequency and distribution of the mutations and their impact on gene expression between the different genes. **B:** Linear regression line between the number of viral variant (x-axis) and the gene length (y-axis). **C:** HeatMap representing the frequency and distribution of the mutations and their impact on gene expression between the different samples. **D:** Linear regression line between the number of frameshift and STOP codon (x-axis) and the viral load expressed in Ct value (y-axis).

Viral variants by gene: S, n=87; N, n=49; ORF3a, n=25; M, n=23; ORF7a, n=10; E, n=8; ORF6, n=6; ORF7b, n=5; ORF8, n=5; ORF10, n=4.

Scale on the right of figures 2A and 2C represents the frequency in percentage, with the largest value in dark and the lowest value in light.

N: number; Ct: cycle threshold, nt: nucleotide; FS: frameshift; STOP: apparition or disappearing of STOP codon

Supplementary Figure 1: Maximum-likelihood phylogenetic trees constructed with PhyML (3.0), GTR model and 1 000 bootstrap resampling. A. nucleotide sequences of the Spike (S) gene**, B.** nucleotide sequences of the Envelope (E) gene, **C.** nucleotide sequences of the Membrane (M) gene, **D.** nucleotide sequences of the Nucleocapsid (NC) gene.

Phylogenetic trees were inferred with the majority consensus sequences for each sample (01292020_NP, 01292020_IS, 01312020_NP, 02012020_NP, 02022020_NP, 02032020_NP, 02042020_NP) and reference sequences issued from NCBI database (MERS-CoV: NC_019843.3, OC43: AY391777.1, HKU1: NC_006577.2, SARS: NC_004718.3, SARS-CoV-2: NC_045512.2 (Wuhan), MT019529.1 (Wuhan), MT019530.1 (Wuhan), MT123290.1 (China), MT049951.1 (China), MT066176.1 (Taiwan), MT007544.1 (Australia), MT292570.1 (Spain), MT093571.1 (Sweden), MT276331.1 (USA), MT126808.1 (Brazil), MT263074.1 (Peru). The patient's sequences are shown in red and the references sequences in black. Nodes presenting a branch support >70% are indicated by an asterisk.

A

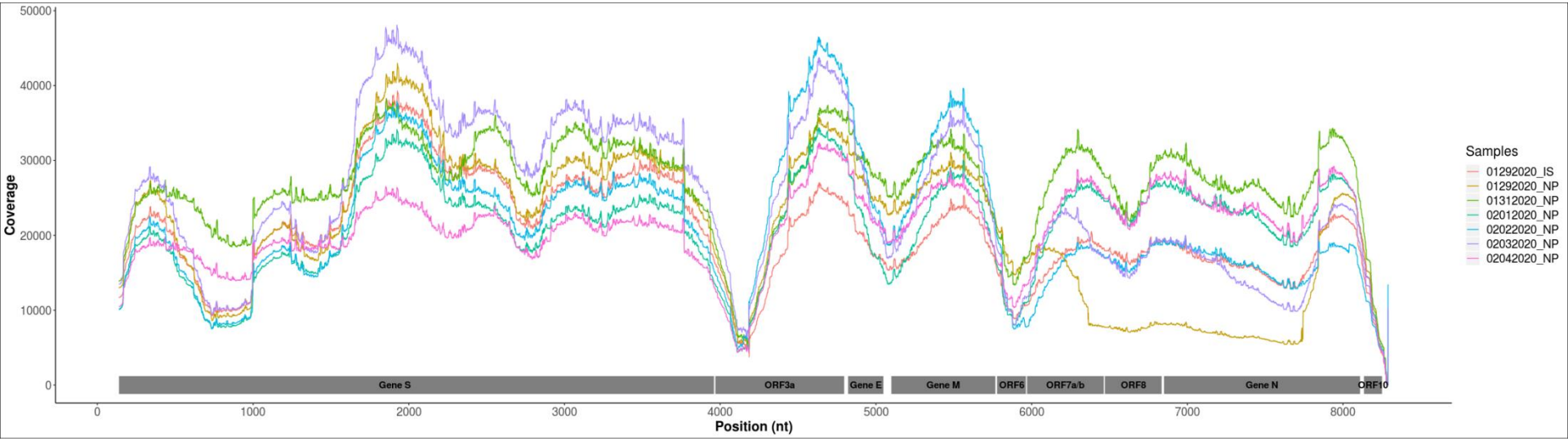
Coverage
50000
40000
30000
20000
10000
0
Gene S
ORF3a
Gene E
Gene M
ORF6
ORF7a/b
ORF8
Gene N
ORF10
0
1000
2000
3000
4000
5000
6000
7000
8000
Position (nt)
Samples
01292020_IS
01292020_NP
01312020_NP
02012020_NP
02022020_NP
02032020_NP
02042020_NP

B

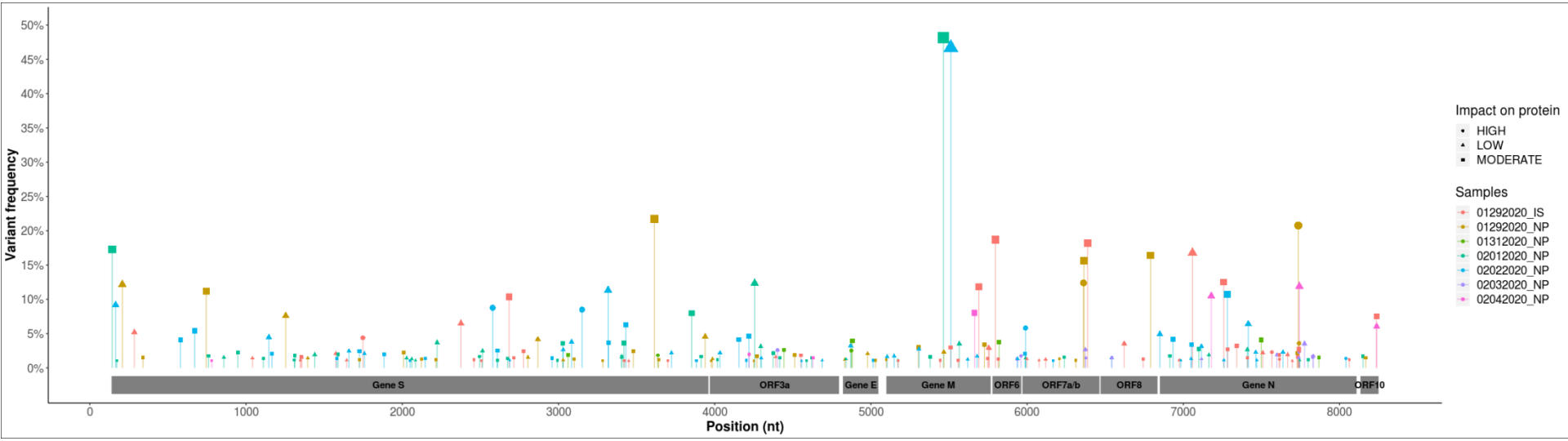
Variant frequency
50%
45%
40%
35%
30%
25%
20%
15%
10%
5%
0%
Gene S
ORF3a
Gene E
Gene M
ORF6
ORF7a/b
ORF8
Gene N
ORF10
0
1000
2000
3000
4000
5000
6000
7000
8000
Position (nt)
Impact on protein
HIGH
LOW
MODERATE
Samples
01292020_IS
01292020_NP
01312020_NP
02012020_NP
02022020_NP
02032020_NP
02042020_NP

A

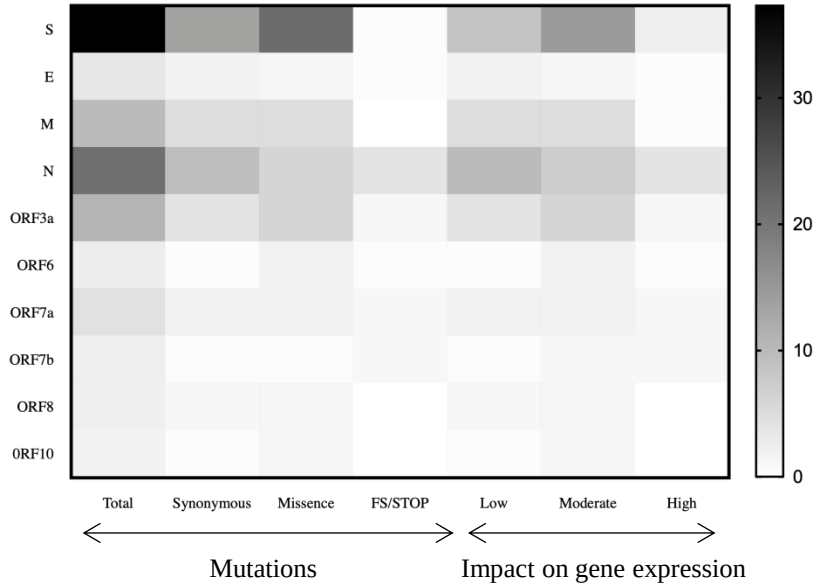
S
E
M
N
ORF3a
ORF6
ORF7a
ORF7b
ORF8
0RF10
30
20
10
0
Total
Synonymous
Missence
FS/STOP
Low
Moderate
High
Mutations
Impact on gene expression

B

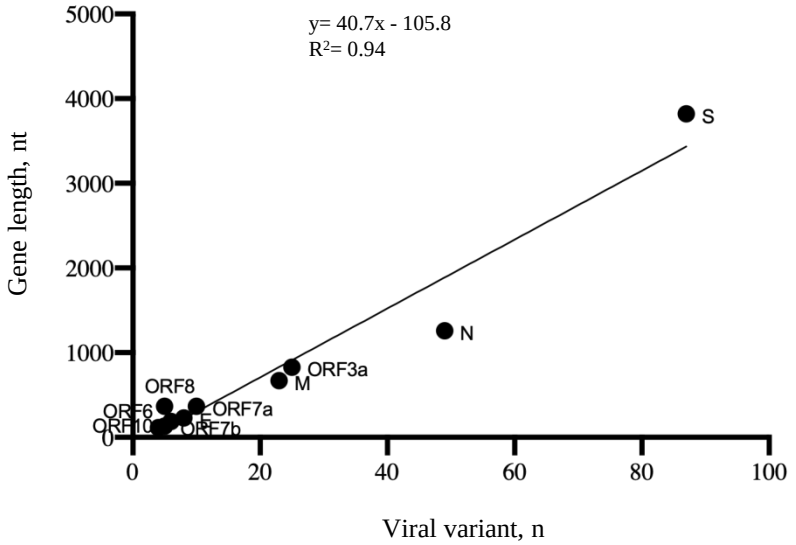
y= 40.7x - 105.8
R²= 0.94
Gene length, nt
5000
4000
3000
2000
1000
0
S
N
ORF3a
M
ORF8
ORF6
ORF7a
ORF7b
0
20
40
60
80
100
Viral variant, n

C

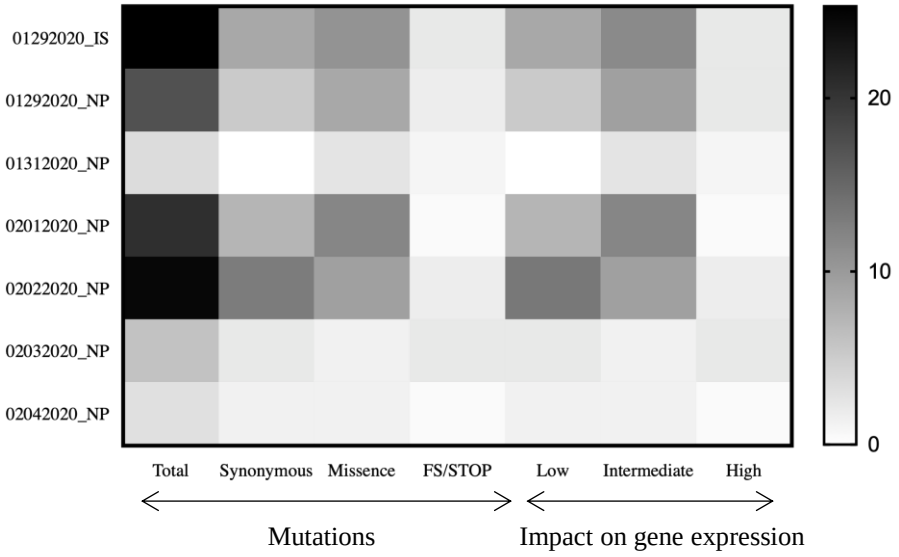
01292020_IS
01292020_NP
01312020_NP
02012020_NP
02022020_NP
02032020_NP
02042020_NP
20
10
0
Total
Synonymous
Missence
FS/STOP
Low
Intermediate
High
Mutations
Impact on gene expression

D

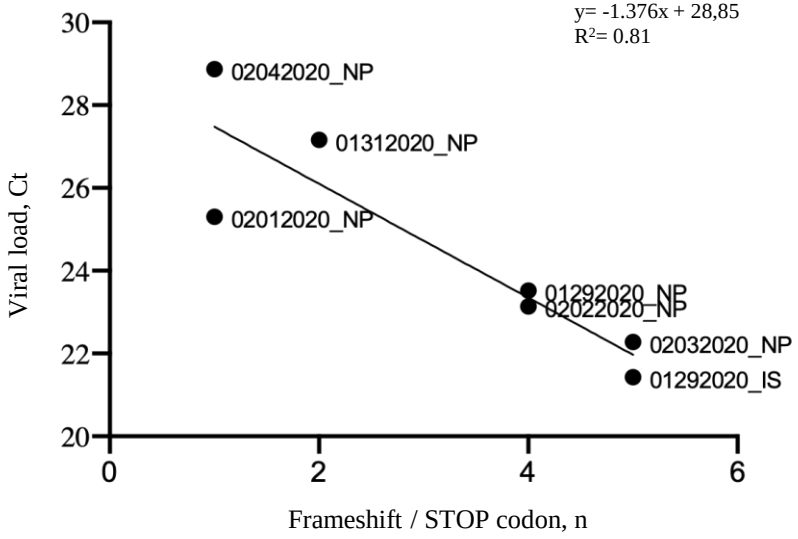
y= -1.376x + 28,85
R²= 0.81
Viral load, Ct
30
28
26
24
22
20
02042020_NP
01312020_NP
02012020_NP
01292020_NP
02022020_NP
02032020_NP
01292020_IS
0
2
4
6
Frameshift / STOP codon, n

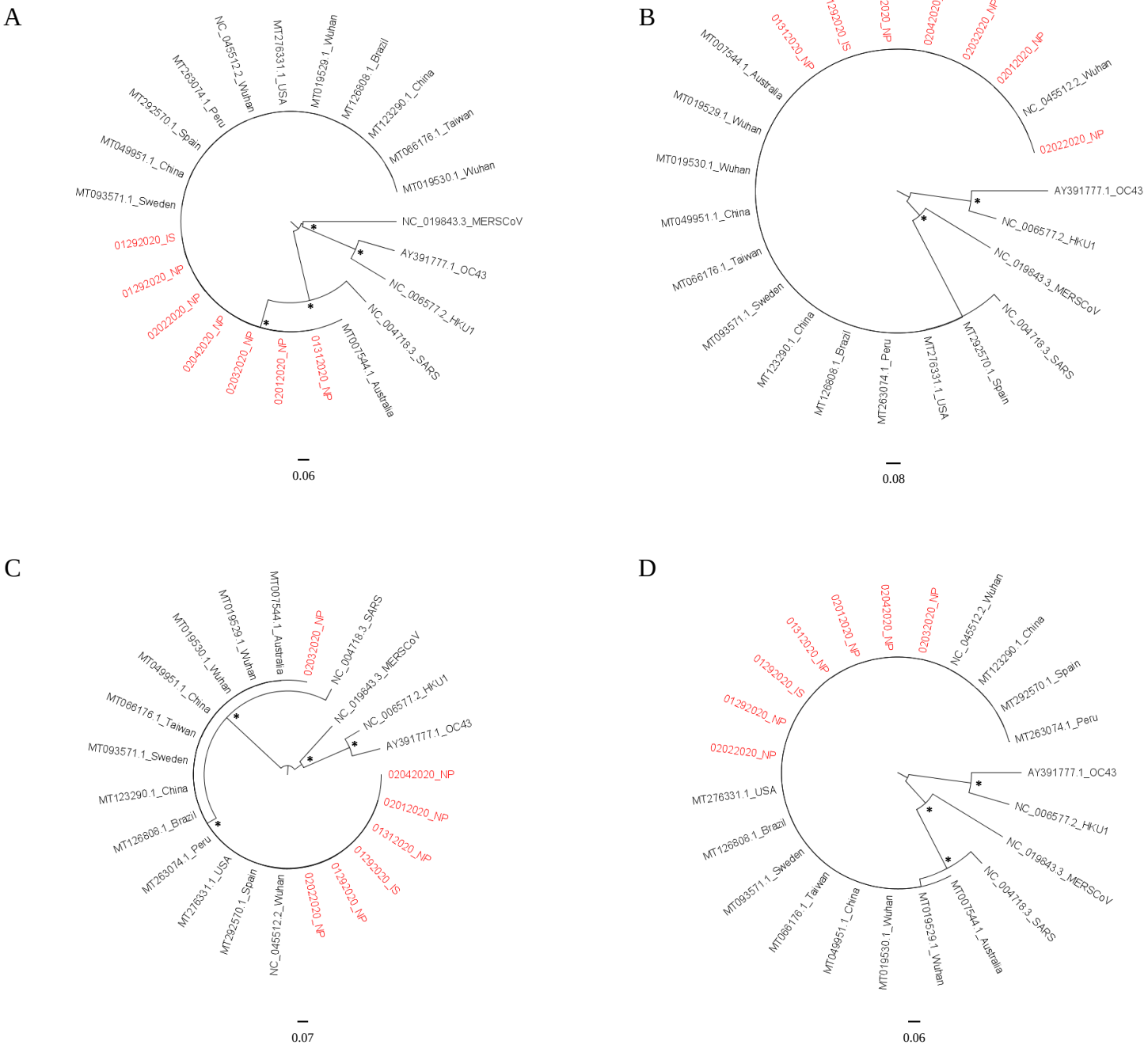
A
NC_045512.2_Wuhan
MT276331.1_USA
MT019529.1_Wuhan
MT126808.1_Brazil
MT123290.1_China
MT066176.1_Taiwan
MT019530.1_Wuhan
MT263074.1_Peru
MT292570.1_Spain
MT049951.1_China
MT093571.1_Sweden
01292020_IS
01292020_NP
02022020_NP
02042020_NP
02032020_NP
02012020_NP
01312020_NP
MT007544.1_Australia
NC_019843.3_MERSCoV
AY391777.1_OC43
NC_006577.2_HKU1
NC_004718.3_SARS
0.06
B
01312020_NP
01292020_IS
01292020_NP
02042020_NP
02032020_NP
02012020_NP
NC_045512.2_Wuhan
02022020_NP
MT007544.1_Australia
MT019529.1_Wuhan
MT019530.1_Wuhan
MT049951.1_China
MT066176.1_Taiwan
MT093571.1_Sweden
MT123290.1_China
MT126808.1_Brazil
MT263074.1_Peru
MT276331.1_USA
MT292570.1_Spain
AY391777.1_OC43
NC_006577.2_HKU1
NC_019843.3_MERSCoV
NC_004718.3_SARS
0.08
C
MT007544.1_Australia
MT019529.1_Wuhan
MT019530.1_Wuhan
MT049951.1_China
MT066176.1_Taiwan
MT093571.1_Sweden
MT123290.1_China
MT126808.1_Brazil
MT263074.1_Peru
MT276331.1_USA
MT292570.1_Spain
NC_045512.2_Wuhan
02032020_NP
NC_004718.3_SARS
NC_019843.3_MERSCoV
NC_006577.2_HKU1
AY391777.1_OC43
02042020_NP
02012020_NP
01312020_NP
01292020_IS
01292020_NP
02022020_NP
0.07
D
02012020_NP
02042020_NP
02032020_NP
NC_045512.2_Wuhan
01312020_NP
MT123290.1_China
01292020_IS
MT292570.1_Spain
01292020_NP
MT263074.1_Peru
02022020_NP
AY391777.1_OC43
MT276331.1_USA
NC_006577.2_HKU1
MT126808.1_Brazil
NC_019843.3_MERSCoV
MT093571.1_Sweden
NC_004718.3_SARS
MT066176.1_Taiwan
MT049951.1_China
MT019530.1_Wuhan
MT019529.1_Wuhan
MT007544.1_Australia
0.06

Supplementary Table 1: Experimental conditions for the amplification of the 2 fragments including the Spike, Envelope, Membrane and Nucleocapsid genes.

		Volume (µl)	Final concentration	PCR program			
	Reverse transcription (Superscript III) 5'- GCAGCTCTCCCTAGCATTGT -3'	-	-	-	-	-	-
	FRAGMENT 1 (4,200 nt)						
First PCR	PrimeSTAR GXL DNA Polymerase	0.5	-	**Initial denaturation**	5 min	98°C	1 cycle
	5X Prime STAR GXL Buffer	5	1X				
	Primer Forward (10µM) 5'-GCATGGTGGACAGCCTTTGT-3'	1	400 nM	**Denaturation**	10s	98°C	
	Primer Reverse (10µM) 5'-TGGGTTTTTGGAACGGCATT-3'	1	400 nM	**Annealing**	15s	60°C	30 cycles
	dNTP Mix (2.5 mM each)	2	-	**Elongation**	5 min	68°C	
	Water PCR grade	13	-				
	Extracted DNA	2.5	-	**Final elongation**	7 min	68°C	1 cycle
	Total	25		**Cooling**		4°C	∞
Nested PCR	PrimeSTAR GXL DNA Polymerase	0.5	-	**Initial denaturation**	5 min	98°C	1 cycle
	5X Prime STAR GXL Buffer	5	1X				
	Primer Forward (10µM) 5'-GGGGTACTGCTGTTATGTCTTT-3'	1	400 nM	**Denaturation**	10s	98°C	
	Primer Reverse (10µM) 5'-CACCCTTGGAGAGTGCTAGT-3'	1	400 nM	**Annealing**	15s	60°C	30 cycles
	dNTP Mix (2.5 mM each)	2	-	**Elongation**	5 min	68°C	
	Water PCR grade	13	-				
	Extracted DNA	2.5	-	**Final elongation**	7 min	68°C	1 cycle
	Total	25		**Cooling**		4°C	∞
	FRAGMENT 2 (4,188 nt)						
First PCR	PrimeSTAR GXL DNA Polymerase	0.5	-	**Initial denaturation**	5 min	98°C	1 cycle
	5X Prime STAR GXL Buffer	5	1X				
	Primer Forward (10µM) 5'- CCGATACAAGCCTCACTCCC-3'	1	400 nM	**Denaturation**	10s	98°C	
	Primer Reverse (10µM) 5'- GCAGCTCTCCCTAGCATTGT-3'	1	400 nM	**Annealing**	15s	60°C	30 cycles
	dNTP Mix (2.5 mM each)	2	-	**Elongation**	5 min	68°C	
	Water PCR grade	13	-				
	Extracted DNA	2.5	-	**Final elongation**	7 min	68°C	1 cycle
	Total	25		**Cooling**		4°C	∞
Nested PCR	PrimeSTAR GXL DNA Polymerase	0.5	-	**Initial denaturation**	5 min	98°C	1 cycle
	5X Prime STAR GXL Buffer	5	1X				
	Primer Forward (10µM) 5'- TGTTGGCGTTGCACTTCTTG-3'	1	400 nM	**Denaturation**	10s	98°C	
	Primer Reverse (10µM) 5'- TGGCTCTTTCAAGTCCTCCC-3'	1	400 nM	**Annealing**	15s	60°C	30 cycles
	dNTP Mix (2.5 mM each)	2	-	**Elongation**	5 min	68°C	
	Water PCR grade	13	-				
	Extracted DNA	2.5	-	**Final elongation**	7 min	68°C	1 cycle
	Total	25		**Cooling**		4°C	∞

nt: nucleotide; DNA: desoxyribonucleic acid; PCR: polymerase chain reaction; min: minute; s: second

Supplementary Table 2: Characteristics of the nasopharyngeal and induced sputum samples with effective amplification and next generation sequencing.

Samples name	Date of sampling	Specimens	Viral load (Ct)	Majority consensus sequence variations	Depth sequencing	No viral variant intra-sample		No viral variant follow-up	
						1%-20%	>20%	1%-20%	>20%
01292020_IS	January, 29th	Induced sputum	21.43	S gene: 3591T>C, Val1197Val	45,773	59	0	59	0
01292020_NP	January, 29th	Nasopharyngeal swab	23.52	S gene: 3591T>C, Val1197Val	39,736	38	2	38	2
01312020_NP	January, 31th	Nasopharyngeal swab	27.16	S gene: 3591T>C, Val1197Val **S gene: 3007delA, Ser1003fs (1008 STOP codon)** **S gene: 3554G>T, Arg1185Leu**	53,081	8	0	8	2
02012020_NP	February, 1st	Nasopharyngeal swab	25.30	S gene: 3591T>C, Val1197Val **S gene: 859G>A, Asp287Asn**	45,523	47	1	47	2
02022020_NP	February, 2nd	Nasopharyngeal swab	23.14	S gene: 3591T> C, Val1197Val	38,397	56	1	56	1
02032020_NP	February, 3rd	Nasopharyngeal swab	22.28	S gene: 3591T>C, Val1197Val	46,274	14	0	14	0
02042020_NP	February, 4th	Nasopharyngeal swab	28.87	S gene: 3591T> C, Val1197Val	42,293	7	0	7	0
				Median [IQR]	45,523 [41,014-46,023]	38 [11-51.5]	0 [0-1]	38 [11-51.5]	1 [1-1.5]

Ct: cycle threshold; del: deletion; fs: frameshift; IQR: interquartile

Non-synonymous mutations are highlighted in bold.

Supplementary Table 3: Characteristics of the 233 intra-sample viral variant identified

Sample	Pos	Depth	Freq	pvalue	Sub	Ins	Del	Prot seq. Modif	Impact on protein	Gene	HGVS.c	HGVS.p	CDS.pos / CDS.length	AA.pos / AA.length
02012020_NP	143	10153	17.3%	0E+00	X			ms	Moderate	S	c.5T>C	p.Phe2Ser	5/3822	2/1273
02022020_NP	165	10873	9.2%	5.7083E-290	X			syn	Low	S	c.27A>G	p.Pro9Pro	27/3822	9/1273
02012020_NP	172	13158	1.1%	5.748E-28	X			ms	Moderate	S	c.34T>C	p.Ser12Pro	34/3822	12/1273
01292020_NP	208	20697	12.1%	0E+00	X			syn	Low	S	c.70T>C	p.Leu24Leu	70/3822	24/1273
01292020_IS	285	21791	5.2%	2.1692E-308	X			syn	Low	S	c.147T>C	p.His49His	147/3822	49/1273
01292020_NP	340	27193	1.5%	1.7248E-90	X			ms	Moderate	S	c.202A>G	p.Met68Val	202/3822	68/1273
02022020_NP	580	14268	4.1%	1.7324E-154	X			ms	Moderate	S	c.442A>G	p.Asn148Asp	442/3822	148/1273
02022020_NP	671	10285	5.4%	2.1195E-153	X			ms	Moderate	S	c.533A>G	p.Asp178Gly	533/3822	178/1273
01292020_NP	745	8882	11.2%	2.9625E-295	X			ms	Moderate	S	c.607A>G	p.Met203Val	607/3822	203/1273
02012020_NP	760	7903	1.8%	3.1608E-33	X			ms	Moderate	S	c.622A>G	p.Thr208Ala	622/3822	208/1273
02042020_NP	781	14396	1.1%	1.0618E-31	X			ms	Moderate	S	c.643G>A	p.Asp215Asn	643/3822	215/1273
02012020_NP	858	7755	1.5%	7.0294E-28	X			syn	Low	S	c.720T>C	p.Thr240Thr	720/3822	240/1273
02012020_NP	947	8918	2.2%	4.9775E-49	X			ms	Moderate	S	c.809T>C	p.Leu270Pro	809/3822	270/1273
01292020_IS	1041	18441	1.4%	2.4564E-57	X			syn	Low	S	c.903T>C	p.Cys301Cys	903/3822	301/1273
02012020_NP	1111	16501	1.4%	6.9683E-51	X			ms	Moderate	S	c.973T>C	p.Ser325Pro	973/3822	325/1273
02022020_NP	1146	17813	4.5%	2.1758E-214	X			syn	Low	S	c.1008C>T	p.Cys336Cys	1008/3822	336/1273
02022020_NP	1166	17894	2.1%	2.1392E-88	X			ms	Moderate	S	c.1028A>G	p.Asn343Ser	1028/3822	343/1273
01292020_NP	1254	19353	7.6%	0E+00	X			syn	Low	S	c.1116A>G	p.Ala372Ala	1116/3822	372/1273
02012020_NP	1309	15936	1.2%	6.2852E-39	X			ms	Moderate	S	c.1171T>C	p.Cys391Arg	1171/3822	391/1273
02012020_NP	1312	16038	1.8%	4.7345E-67	X			ms	Moderate	S	c.1174T>C	p.Phe392Leu	1174/3822	392/1273
01292020_IS	1347	19015	1.1%	2.063E-42	X			syn	Low	S	c.1209A>G	p.Ter403Ter	1209/3822	403/1273
01292020_IS	1355	19013	1.6%	1.9594E-69	X			ms	Moderate	S	c.1217A>G	p.Glu406Gly	1217/3822	406/1273
01292020_IS	1356	19074	1.6%	8.0772E-66	X			syn	Low	S	c.1218A>G	p.Glu406Glu	1218/3822	406/1273
01292020_NP	1395	16647	1.4%	2.9423E-52	X			syn	Low	S	c.1257T>C	p.Ala419Ala	1257/3822	419/1273
02012020_NP	1440	16352	2.0%	3.0554E-75	X			syn	Low	S	c.1302A>G	p.Met434Met	1302/3822	434/1273
01292020_IS	1575	24299	2.1%	1.1824E-119	X			syn	Low	S	c.1437T>C	p.Pro479Pro	1437/3822	479/1273

02022020_NP	1580	21350	1.3%	2.9888E-61	X	ms	Moderate	S	c.1442A>G	p.Asn481Ser	1442/3822	481/1273
0201202à_NP	1589	19557	2.0%	1.1015E-89	X	ms	Moderate	S	c.1451A>G	p.Glu484Gly	1451/3822	484/1273
0129202à_IS	1644	26537	1.1%	4.1775E-61	X	syn	Low	S	c.1506T>C	p.Gly502Gly	1506/3822	502/1273
02022020_NP	1659	27912	2.4%	7.956E-167	X	syn	Low	S	c.1521A>G	p.Pro507Pro	1521/3822	507/1273
01292020_NP	1726	34596	1.2%	5.2313E-83	X	ms	Moderate	S	c.1588T>C	p.Ser530Pro	1588/3822	530/1273
02022020_NP	1726	30839	2.4%	1.5696E-181	X	ms	Moderate	S	c.1588T>C	p.Ser530Pro	1588/3822	530/1273
01292020_IS	1748	33208	4.4%	0E+00	X	+stop	High	S	c.1610A>G	p.Lys537*	1610/3822	537/1273
02022020_NP	1758	31453	2.1%	1.0244E-153	X	syn	Low	S	c.1620T>C	p.Asn540Asn	1620/3822	540/1273
02022020_NP	1883	36160	2.0%	1.3989E-168	X	ms	Moderate	S	c.1745T>C	p.Leu582Pro	1745/3822	582/1273
01292020_NP	2008	40843	2.3%	2.4157E-223	X	ms	Moderate	S	c.1870A>G	p.Ile624Val	1870/3822	624/1273
02012020_NP	2028	32383	1.4%	8.5419E-101	X	syn	Low	S	c.1890T>C	p.Thr630Thr	1890/3822	630/1273
02022020_NP	2050	35251	1.1%	1.7906E-74	X	ms	Moderate	S	c.1912A>G	p.Thr638Ala	1912/3822	638/1273
02012020_NP	2061	31722	1.3%	3.6477E-90	X	syn	Low	S	c.1923T>C	p.Asn641Asn	1923/3822	641/1273
02012020_NP	2085	32064	1.1%	3.4148E-70	X	syn	Low	S	c.1947T>C	p.Cys649Cys	1947/3822	649/1273
01292020_NP	2122	37192	1.3%	4.8206E-98	X	ms	Moderate	S	c.1984T>C	p.Cys662Arg	1984/3822	662/1273
02022020_NP	2147	31047	1.4%	8.1127E-92	X	ms	Moderate	S	c.2009T>C	p.Met670Thr	2009/3822	670/1273
01292020_NP	2216	32392	1.2%	6.7386E-81	X	ms	Moderate	S	c.2078T>C	p.Ile693Thr	2078/3822	693/1273
02012020_NP	2223	27675	3.7%	2.1472E-264	X	syn	Low	S	c.2085C>T	p.Tyr695Tyr	2085/3822	695/1273
01292020_IS	2376	28641	6.5%	0E+00	X	syn	Low	S	c.2238A>G	p.Ser746Ser	2238/3822	746/1273
01292020_IS	2459	28789	1.2%	2.3146E-72	X	ms	Moderate	S	c.2321A>G	p.Gln774Arg	2321/3822	774/1273
02012020_NP	2495	24039	1.7%	2.7785E-90	X	+stop	High	S	c.2357A>G	p.Lys786*	2357/3822	786/1273
01292020_IS	2509	28643	1.0%	3.3537E-58	X	ms	Moderate	S	c.2371A>G	p.Thr791Ala	2371/3822	791/1273
02012020_NP	2514	23629	2.5%	4.9453E-142	X	syn	Low	S	c.2376A>G	p.Pro792Pro	2376/3822	792/1273
02022020_NP	2579	25373	8.8%	0E+00	X	+stop	High	S	c.2441A>G	p.Lys814*	2441/3822	814/1273
02012020_NP	2609	22107	1.1%	6.8278E-50	X	ms	Moderate	S	c.2471A>G	p.Asn824Ser	2471/3822	824/1273
02022020_NP	2609	23895	2.5%	3.9353E-150	X	ms	Moderate	S	c.2471A>G	p.Asn824Ser	2471/3822	824/1273
02012020_NP	2674	20228	1.4%	3.8664E-62	X	ms	Moderate	S	c.2536G>A	p.Ala846Thr	2536/3822	846/1273
01292020_IS	2684	23647	10.4%	0E+00	X	ms	Moderate	S	c.2546T>C	p.Leu849Pro	2546/3822	849/1273
02022020_NP	2688	20909	1.1%	7.1363E-46	X	syn	Low	S	c.2550T>C	p.Ile850Ile	2550/3822	850/1273
01292020_IS	2714	22259	1.5%	3.0942E-70	X	ms	Moderate	S	c.2576C>T	p.Thr859Ile	2576/3822	859/1273
01292020_IS	2776	21710	2.4%	3.5615E-128	X	ms	Moderate	S	c.2638G>A	p.Gly880Ser	2638/3822	880/1273

01292020_NP	2805	22965	1.6%	1.8027E-80	X	syn	Low	S	c.2667T>C	p.Gly889Gly	2667/3822	889/1273
01292020_NP	2868	26300	4.2%	1.9715E-290	X	syn	Low	S	c.2730A>G	p.Gly910Gly	2730/3822	910/1273
02022020_NP	2959	25791	1.4%	6.8174E-80	X	ms	Moderate	S	c.2821A>G	p.Thr941Ala	2821/3822	941/1273
02012020_NP	2993	22792	1.1%	1.1015E-50	X	ms	Moderate	S	c.2855T>C	p.Val952Ala	2855/3822	952/1273
02012020_NP	3028	24008	3.6%	1.1571E-222	X	ms	Moderate	S	c.2890A>G	p.Lys964Glu	2890/3822	964/1273
01292020_NP	3030	30260	1.2%	1.5916E-71	X	syn	Low	S	c.2892A>G	p.Lys964Lys	2892/3822	964/1273
02022020_NP	3030	27014	2.6%	7.4876E-176	X	syn	Low	S	c.2892A>G	p.Lys964Lys	2892/3822	964/1273
01312020_NP	3061	34285	1.9%	1.3815E-146	X	ms	Moderate	S	c.2923A>G	p.Ser975Gly	2923/3822	975/1273
02022020_NP	3084	27242	3.8%	2.4935E-268	X	syn	Low	S	c.2946A>G	p.Ser982Ser	2946/3822	982/1273
01292020_NP	3101	30083	1.3%	3.5007E-80	X	ms	Moderate	S	c.2963A>T	p.Glu988Val	2963/3822	988/1273
02022020_NP	3151	26391	8.5%	0E+00	X	+stop	High	S	c.3013C>T	p.Gln1005*	3013/3822	1005/1273
01292020_NP	3284	29684	1.0%	7.2714E-61	X	ms	Moderate	S	c.3146T>C	p.Leu1049Pro	3146/3822	1049/1273
02022020_NP	3318	27872	11.3%	0E+00	X	syn	Low	S	c.3180A>G	p.Val1060Val	3180/3822	1060/1273
02022020_NP	3320	28389	3.7%	1.8375E-270	X	ms	Moderate	S	c.3182T>G	p.Val1061Gly	3182/3822	1061/1273
02012020_NP	3404	24030	1.6%	1.1719E-86	X	ms	Moderate	S	c.3266T>C	p.Phe1089Ser	3266/3822	1089/1273
02012020_NP	3405	23991	1.6%	5.3895E-89	X	syn	Low	S	c.3267T>C	p.Phe1089Phe	3267/3822	1089/1273
02012020_NP	3419	23839	3.6%	3.772E-225	X	ms	Moderate	S	c.3281T>C	p.Val1094Ala	3281/3822	1094/1273
01292020_IS	3421	28286	1.1%	8.6034E-60	X	ms	Moderate	S	c.3283T>G	p.Phe1095Val	3283/3822	1095/1273
02022020_NP	3431	26850	6.3%	0E+00	X	ms	Moderate	S	c.3293A>G	p.Asn1098Ser	3293/3822	1098/1273
01292020_IS	3450	29153	1.0%	1.7008E-58	X	syn	Low	S	c.3312A>G	p.Val1104Val	3312/3822	1104/1273
01292020_NP	3479	31053	2.5%	1.7669E-186	X	ms	Moderate	S	c.3341T>C	p.Ile1114Thr	3341/3822	1114/1273
01292020_NP	3614	30845	21.7%	0E+00	X	ms	Moderate	S	c.3476A>G	p.His1159Arg	3476/3822	1159/1273
01312020_NP	3636	29596	1.9%	7.3643E-127	X	-stop	High	S	c.3497A>G	p.Ter1166Trpext*?	3497/3822	1166/1273
01292020_NP	3641	28685	1.2%	1.784E-70	X	ms	Moderate	S	c.3503A>G	p.Asp1168Gly	3503/3822	1168/1273
01292020_IS	3700	28435	1.0%	1.8167E-58	X	ms	Moderate	S	c.3562G>A	p.Glu1188Lys	3562/3822	1188/1273
02022020_NP	3723	24864	2.2%	2.3637E-129	X	syn	Low	S	c.3585A>G	p.Glu1195Glu	3585/3822	1195/1273
02012020_NP	3853	18568	8.0%	0E+00	X	ms	Moderate	S	c.3715A>G	p.Ser1239Gly	3715/3822	1239/1273
02022020_NP	3883	19176	1.1%	5.031E-40	X	ms	Moderate	S	c.3745T>C	p.Ser1249Pro	3745/3822	1249/1273
02012020_NP	3914	16757	1.7%	2.2287E-63	X	ms	Moderate	S	c.3776A>G	p.Asp1259Gly	3776/3822	1259/1273
01292020_NP	3939	19040	4.6%	5.3194E-234	X	syn	Low	S	c.3801A>G	p.Gly1267Gly	3801/3822	1267/1273
01292020_NP	3978	17011	1.0%	1.2179E-33	X	ms	Moderate	ORF3a	c.10T>C	p.Phe4Leu	10/828	4/275

01292020_NP	3986	16202	1.3%	5.8624E-46	X		syn	Low	ORF3a	c.18A>G	p.Ter6Ter	18/828	6/275
02012020_NP	4018	11400	1.2%	1.771E-28	X		ms	Moderate	ORF3a	c.50A>G	p.Gln17Arg	50/828	17/275
02022020_NP	4034	11803	2.2%	8.6459E-64	X		syn	Low	ORF3a	c.66T>C	p.Asp22Asp	66/828	22/275
02022020_NP	4155	6265	4.2%	2.9108E-70	X		ms	Moderate	ORF3a	c.187A>G	p.Met63Val	187/828	63/275
02022020_NP	4203	11874	1.1%	2.136E-27	X		ms	Moderate	ORF3a	c.235T>C	p.Phe79Leu	235/828	79/275
02022020_NP	4219	13091	4.6%	2.1749E-162	X		ms	Moderate	ORF3a	c.251T>C	p.Leu84Pro	251/828	84/275
02042020_NP	4220	8907	2.0%	5.3772E-43		X	fs	High	ORF3a	c.255_283delGTTGTTTGTAA CAGTTTACTCACACCTTT	p.Leu85fs	255/828	85/275
01292020_NP	4251	13136	1.0%	6.529E-27	X		syn	Low	ORF3a	c.283T>C	p.Leu95Leu	283/828	95/275
02012020_NP	4256	12285	12.3%	0E+00	X		syn	Low	ORF3a	c.288C>T	p.Leu96Leu	288/828	96/275
01292020_NP	4270	14064	1.7%	5.4529E-55	X		ms	Moderate	ORF3a	c.302T>C	p.Leu101Pro	302/828	101/275
02012020_NP	4295	14803	3.1%	1.4641E-117	X		syn	Low	ORF3a	c.327T>C	p.Tyr109Tyr	327/828	109/275
02022020_NP	4298	20657	1.4%	8.8179E-64	X		syn	Low	ORF3a	c.330T>C	p.Ala110Ala	330/828	110/275
02012020_NP	4374	20962	2.2%	2.7973E-108	X		ms	Moderate	ORF3a	c.406A>G	p.Lys136Glu	406/828	136/275
01292020_IS	4391	17332	1.6%	2.6205E-61	X		syn	Low	ORF3a	c.423T>C	p.Tyr141Tyr	423/828	141/275
02032020_NP	4402	27230	2.6%	4.044E-174		X	fs	High	ORF3a	c.435_438delTTTT	p.Leu147fs	435/828	145/275
02012020_NP	4417	22555	1.5%	6.9564E-72	X		ms	Moderate	ORF3a	c.449A>G	p.His150Arg	449/828	150/275
01312020_NP	4443	28821	2.6%	2.3252E-185	X		ms	Moderate	ORF3a	c.475C>T	p.Pro159Ser	475/828	159/275
01292020_NP	4513	30487	1.9%	1.9039E-135	X		ms	Moderate	ORF3a	c.545A>G	p.His182Arg	545/828	182/275
01292020_IS	4551	22658	1.8%	9.3095E-97	X		ms	Moderate	ORF3a	c.583T>C	p.Ser195Pro	583/828	195/275
02022020_NP	4556	39633	1.0%	3.3479E-77	X		syn	Low	ORF3a	c.588A>G	p.Gly196Gly	588/828	196/275
02012020_NP	4588	31322	1.0%	1.6809E-62	X		ms	Moderate	ORF3a	c.620T>C	p.Phe207Ser	620/828	207/275
02012020_NP	4621	32896	1.4%	5.4691E-103	X		ms	Moderate	ORF3a	c.653A>G	p.Gln218Arg	653/828	218/275
02042020_NP	4629	31880	1.5%	2.6992E-105	X		ms	Moderate	ORF3a	c.661A>G	p.Thr221Ala	661/828	221/275
02022020_NP	4688	45488	1.1%	2.1176E-97	X		syn	Low	ORF3a	c.720T>C	p.Pro240Pro	720/828	240/275
01292020_NP	4832	30787	1.2%	4.3473E-76	X		syn	Low	E	c.12C>T	p.Phe4Phe	12/228	4/75
02012020_NP	4841	27869	1.3%	4.147E-75	X		syn	Low	E	c.21A>G	p.Glu7Glu	21/228	7/75
02022020_NP	4871	32976	3.2%	2.273E-271	X		syn	Low	E	c.51A>G	p.Val17Val	51/228	17/75
01312020_NP	4875	30850	2.5%	2.2483E-191	X		fs	High	E	c.60dupT	p.Leu21fs	61/228	21/75
01312020_NP	4881	30018	4.0%	9.3266E-313	X		ms	Moderate	E	c.61C>T	p.Leu21Phe	61/228	21/75
01292020_NP	4979	24878	2.1%	4.684E-121	X		syn	Low	E	c.159A>G	p.Lys53Lys	159/228	53/75
02022020_NP	5014	22934	1.1%	1.487E-52	X		ms	Moderate	E	c.194T>C	p.Leu65Pro	194/228	65/75

01292020_NP	5029	24454	1.1%	1.0712E-54	X	ms	Moderate	E	c.209T>C	p.Val70Ala	209/228	70/75
02012020_NP	5071	14177	5.6%	8.3642E-218	X	non coding	-	M	c.-28T>C			
01292020_NP	5084	22783	1.8%	8.3807E-93	X	non coding	-	M	c.-15A>G			
02032020_NP	5087	17014	1.4%	9.8893E-50	X	non coding	-	M	c.-12T>C			
01292020_IS	5092	15779	8.6%	0E+00	X	non coding	-	M	c.-7T>C			
01292020_NP	5099	22852	1.2%	1.372E-56	X	Start lost	High	M	c.1A>C	p.Met1?	1/669	1/222
02022020_NP	5104	18922	1.7%	1.6914E-71	X	syn	Low	M	c.6A>G	p.Ala2Ala	6/669	2/222
02022020_NP	5149	20579	1.7%	1.9445E-82	X	syn	Low	M	c.51T>C	p.Leu17Leu	51/669	17/222
02012020_NP	5173	15735	1.1%	5.6504E-36	X	syn	Low	M	c.75T>C	p.Gly25Gly	75/669	25/222
01292020_IS	5175	16726	1.1%	3.006E-36	X	ms	Moderate	M	c.77T>C	p.Phe26Ser	77/669	26/222
01292020_NP	5304	26859	3.0%	1.8549E-207	X	ms	Moderate	M	c.206C>T	p.Ala69Val	206/669	69/222
02022020_NP	5308	30125	2.7%	1.8189E-202	X	syn	Low	M	c.210T>C	p.Val70Val	210/669	70/222
02012020_NP	5379	25273	1.6%	1.5247E-91	X	ms	Moderate	M	c.281G>A	p.Ser94Asn	281/669	94/222
01292020_IS	5444	22587	1.1%	3.2035E-51	X	ms	Moderate	M	c.346A>G	p.Thr116Ala	346/669	116/222
02012020_NP	5465	28153	48.2%	0E+00	X	ms	Moderate	M	c.367C>T	p.Pro123Ser	367/669	123/222
01292020_NP	5467	29260	2.3%	7.7569E-165	X	syn	Low	M	c.369A>C	p.Pro123Pro	369/669	123/222
01292020_IS	5511	23455	3.0%	9.9295E-177	X	ms	Moderate	M	c.413T>C	p.Leu138Pro	413/669	138/222
02022020_NP	5512	37912	46.7%	0E+00	X	syn	Low	M	c.414C>T	p.Leu138Leu	414/669	138/222
01292020_IS	5559	23687	1.1%	9.3103E-52	X	ms	Moderate	M	c.461A>G	p.His154Arg	461/669	154/222
02012020_NP	5566	29886	3.5%	4.7456E-271	X	syn	Low	M	c.468A>G	p.Leu156Leu	468/669	156/222
02022020_NP	5620	34716	1.3%	5.0802E-90	X	syn	Low	M	c.522A>G	p.Arg174Arg	522/669	174/222
02042020_NP	5664	23869	8.0%	0E+00	X	ms	Moderate	M	c.566G>A	p.Gly189Asp	566/669	189/222
02022020_NP	5680	31895	1.7%	2.0298E-123	X	syn	Low	M	c.582T>C	p.Ala194Ala	582/669	194/222
01292020_IS	5691	20823	11.8%	0E+00	X	ms	Moderate	M	c.593G>A	p.Arg198His	593/669	198/222
01292020_NP	5727	24055	3.4%	1.277E-209	X	ms	Moderate	M	c.629A>G	p.His210Arg	629/669	210/222
01292020_IS	5748	17579	1.4%	1.4734E-53	X	ms	Moderate	M	c.650T>C	p.Ile217Thr	650/669	217/222
01292020_IS	5753	17221	2.9%	2.9916E-127	X	syn	Low	M	c.655T>C	p.Leu219Leu	655/669	219/222
01292020_IS	5758	17186	2.9%	1.8926E-123	X	syn	Low	M	c.660T>C	p.Leu220Leu	660/669	220/222
01292020_IS	5773	15670	9.3%	0E+00	X	non coding	-	ORF6	c.-5A>G			
01292020_IS	5797	14988	18.7%	0E+00	X	ms	Moderate	ORF6	c.20T>A	p.Phe7Tyr	20/186	6/61
01292020_IS	5815	11765	1.3%	1.2297E-33	X	ms	Moderate	ORF6	c.38A>G	p.Glu13Gly	38/186	13/61

01312020_NP	5821	17614	3.7%	2.4982E-173	X		ms	Moderate	ORF6	c.44T>C	p.Leu15Ser	44/186	15/61
02032020_NP	5937	10555	1.3%	1.3761E-29	X		ms	Moderate	ORF6	c.160G>A	p.Glu54Lys	160/186	54/61
02022020_NP	5939	8469	1.4%	7.4125E-26	X		syn	Low	ORF6	c.162A>G	p.Glu54Glu	162/186	54/61
02032020_NP	5961	11849	1.8%	1.1352E-48		X	fs	High	ORF6	c.184_185insTCTCC	p.Ter62fs	185/186	62/61
02022020_NP	5988	8378	2.1%	7.0965E-42	X		ms	Moderate	ORF7a	c.19T>A	p.Leu7Met	19/366	7/121
02012020_NP	5990	11840	1.4%	3.2719E-37	X		syn	Low	ORF7a	c.21G>A	p.Leu7Leu	21/366	7/121
02022020_NP	5990	8696	5.8%	1.401E-141		X	fs	High	ORF7a	c.21_22insA	p.Ala8fs	22/366	8/121
01292020_IS	5999	12072	1.3%	1.3281E-33	X		syn	Low	ORF7a	c.30A>G	p.Met10Met	30/366	10/121
01292020_IS	6077	14467	1.1%	3.1214E-32	X		syn	Low	ORF7a	c.108T>C	p.Ser36Ser	108/366	36/121
01292020_IS	6119	15505	1.3%	1.2165E-41	X		syn	Low	ORF7a	c.150T>C	p.Ala50Ala	150/366	50/121
02022020_NP	6166	15235	1.0%	5.4631E-32	X		ms	Moderate	ORF7a	c.197C>T	p.Ala66Val	197/366	66/121
01292020_NP	6207	16759	1.3%	2.08E-48	X		-stop	High	ORF7a	c.238A>G	p.Ter80Glyext*?	238/366	80/121
02012020_NP	6238	25319	1.5%	5.5449E-86	X		ms	Moderate	ORF7a	c.269A>G	p.Gln90Arg	269/366	90/121
01292020_NP	6312	12311	1.1%	1.1185E-27	X		ms	Moderate	ORF7a	c.343A>G	p.Thr115Ala	343/366	115/121
01292020_NP	6361	10377	12.4%	0E+00		X	fs	High	ORF7b	c.31_32insCAAACAT	p.Leu11fs	32/132	10/43
01292020_NP	6364	9620	15.6%	0E+00		X	Conservative inframe	Moderate	ORF7b	c.33_34insGCCGCAAAT	p.Leu11_Cys12insAlaAlaAsn	34/132	11/43
02032020_NP	6373	19491	2.7%	1.4772E-128	X		syn	Low	ORF7b	c.42A>G	p.Leu14Leu	42/132	14/43
02032020_NP	6376	19374	1.4%	4.0553E-61		X	fs	High	ORF7b	c.45_46insGCAAATTGCACAA	p.Phe16fs	46/132	16/43
01292020_IS	6387	20212	18.2%	0E+00	X		ms	Moderate	ORF7b	c.56T>C	p.Phe19Ser	56/132	19/43
02022020_NP	6541	16595	1.5%	1.2223E-53	X		syn	Low	ORF8	c.72A>G	p.Ser24Ser	72/366	24/121
02032020_NP	6543	16338	1.5%	1.5365E-52	X		ms	Moderate	ORF8	c.74G>T	p.Cys25Phe	74/366	25/121
01292020_IS	6622	16391	3.5%	1.4242E-151	X		syn	Low	ORF8	c.153T>C	p.Ala51Ala	153/366	51/121
01292020_IS	6743	17832	1.3%	1.5444E-50	X		ms	Moderate	ORF8	c.274G>A	p.Glu92Lys	274/366	92/121
01292020_NP	6791	8376	16.4%	0E+00	X		ms	Moderate	ORF8	c.322T>C	p.Phe108Leu	322/366	108/121
02022020_NP	6850	19211	4.9%	1.4773E-257	X		Initiator codon variant	Low	N	c.1A>G	p.Met1?	1/1260	1/419
02012020_NP	6914	26656	1.8%	8.6251E-107	X		ms	Moderate	N	c.65A>G	p.Asp22Gly	65/1260	22/419
02022020_NP	6934	19286	4.2%	3.4338E-213	X		ms	Moderate	N	c.85A>G	p.Asn29Asp	85/1260	29/419
01292020_IS	6975	18251	1.2%	3.3193E-43	X		syn	Low	N	c.126C>T	p.Pro42Pro	126/1260	42/419
02022020_NP	6984	18556	1.1%	1.5645E-40	X		syn	Low	N	c.135A>G	p.Leu45Leu	135/1260	45/419
02022020_NP	7050	18173	1.3%	7.3496E-52	X		syn	Low	N	c.201T>C	p.Pro67Pro	201/1260	67/419
02022020_NP	7052	18200	3.4%	1.4062E-161	X		ms	Moderate	N	c.203G>A	p.Arg68Gln	203/1260	68/419

01292020_IS	7059	17703	16.8%	0E+00	X		syn	Low	N	c.210A>G	p.Gln70Gln	210/1260	70/419
02012020_NP	7099	24182	2.8%	2.6753E-167	X		ms	Moderate	N	c.250A>G	p.Ile84Val	250/1260	84/419
02022020_NP	7116	17704	3.1%	6.7922E-142	X		syn	Low	N	c.267A>G	p.Ter89Ter	267/1260	89/419
02032020_NP	7116	16921	1.3%	1.3854E-47	X		syn	Low	N	c.267A>G	p.Ter89Ter	267/1260	89/419
02012020_NP	7164	24407	1.9%	1.8958E-105	X		syn	Low	N	c.315T>C	p.Ser105Ser	315/1260	105/419
02042020_NP	7179	25326	10.5%	0E+00	X		syn	Low	N	c.330C>T	p.Phe110Phe	330/1260	110/419
01292020_IS	7259	16469	12.5%	0E+00	X		ms	Moderate	N	c.410G>A	p.Gly137Glu	410/1260	137/419
02022020_NP	7260	16636	1.1%	1.8589E-39	X		syn	Low	N	c.411A>G	p.Gly137Gly	411/1260	137/419
02022020_NP	7282	16758	10.7%	0E+00	X		ms	Moderate	N	c.433C>T	p.His145Tyr	433/1260	145/419
01292020_IS	7283	15853	2.7%	8.9471E-108	X		ms	Moderate	N	c.434A>G	p.His145Arg	434/1260	145/419
01292020_IS	7342	15999	3.2%	1.2872E-133	X		ms	Moderate	N	c.493A>G	p.Thr165Ala	493/1260	165/419
02012020_NP	7410	23238	2.7%	4.4022E-153	X		syn	Low	N	c.561A>G	p.Ser187Ser	561/1260	187/419
01292020_IS	7411	15973	1.5%	1.6423E-51	X		ms	Moderate	N	c.562T>C	p.Ser188Pro	562/1260	188/419
02022020_NP	7416	16062	6.4%	3.7923E-288	X		syn	Low	N	c.567T>C	p.Arg189Arg	567/1260	189/419
02022020_NP	7464	15493	2.3%	1.789E-85	X		syn	Low	N	c.615T>C	p.Thr205Thr	615/1260	205/419
02022020_NP	7470	15401	1.1%	3.0227E-36	X		syn	Low	N	c.621T>C	p.Pro207Pro	621/1260	207/419
01312020_NP	7499	26214	4.1%	9.3557E-282	X		ms	Moderate	N	c.650C>T	p.Ala217Val	650/1260	217/419
01292020_IS	7509	14683	2.2%	2.1121E-79	X		syn	Low	N	c.660T>C	p.Ala220Ala	660/1260	220/419
01292020_IS	7567	13890	2.3%	8.4292E-79	X		+stop	High	N	c.718C>T	p.Gln240*	718/1260	240/419
02032020_NP	7599	10602	1.9%	1.0042E-47	X		syn	Low	N	c.750T>C	p.Ser250Ser	750/1260	250/419
01292020_IS	7615	14022	1.9%	9.5012E-63	X		ms	Moderate	N	c.766A>C	p.Lys256Gln	766/1260	256/419
01292020_IS	7616	13996	1.3%	1.884E-38	X		+stop	High	N	c.767A>G	p.Lys256*	767/1260	256/419
02022020_NP	7638	12989	2.3%	6.9487E-74	X		syn	Low	N	c.789T>C	p.Thr263Thr	789/1260	263/419
01292020_IS	7668	12915	1.9%	7.9435E-60	X		syn	Low	N	c.819T>C	p.Ala273Ala	819/1260	273/419
01292020_IS	7698	13047	1.0%	1.1943E-26	X		syn	Low	N	c.849A>G	p.Gln283Gln	849/1260	283/419
01292020_NP	7729	6034	2.2%	2.5706E-32		X	Disruptive inframe	Moderate	N	c.881_882insGAATGA	p.Gln294_Gly295insAsnGlu	882/1260	294/419
01292020_IS	7731	14110	1.6%	4.4317E-51		X	Conservative inframe	Moderate	N	c.882_883insATT	p.Gln294_Gly295insIle	883/1260	295/419
01292020_NP	7736	7613	20.8%	0E+00		X	fs	High	N	c.888_889insTT	p.Asp297fs	889/1260	297/419
01292020_IS	7739	14577	2.8%	3.7126E-101		X	Disruptive inframe	Moderate	N	c.890_891insCTTGCT	p.Asp297_Tyr298insLeuLeu	891/1260	297/419
02032020_NP	7739	11045	1.4%	3.4276E-36		X	fs	High	N	c.890_891insCTTCTATT TGTGCTTT	p.Tyr298fs	891/1260	297/419

01292020_NP	7741	6212	3.6%	3.2415E-59			X	fs	High	N	c.893delA	p.Tyr298fs	893/1260	298/419
02032020_NP	7741	11064	2.4%	7.8635E-64		X		fs	High	N	c.892_893insGA	p.Tyr298fs	893/1260	298/419
01292020_IS	7742	14676	2.6%	2.7903E-93		X		fs	High	N	c.893_894insG	p.Tyr298fs	894/1260	298/419
02042020_NP	7743	22632	11.9%	0E+00	X			syn	Low	N	c.894C>T	p.Tyr298Tyr	894/1260	298/419
02012020_NP	7746	20441	1.1%	2.7888E-44	X			syn	Low	N	c.897A>G	p.Lys299Lys	897/1260	299/419
02032020_NP	7776	12993	3.5%	2.8664E-120	X			syn	Low	N	c.927C>T	p.Pro309Pro	927/1260	309/419
02012020_NP	7799	21837	1.2%	6.5089E-54	X			ms	Moderate	N	c.950T>C	p.Met317Thr	950/1260	317/419
02032020_NP	7829	16721	1.6%	2.0235E-61	X			ms	Moderate	N	c.980C>T	p.Ser327Leu	980/1260	327/419
02032020_NP	7833	16714	1.7%	4.9661E-67	X			syn	Low	N	c.984A>G	p.Gly328Gly	984/1260	328/419
01312020_NP	7868	31788	1.5%	2.6863E-105	X			ms	Moderate	N	c.1019A>G	p.Asp340Gly	1019/1260	340/419
02022020_NP	8041	17844	1.4%	7.8876E-54		X		fs	High	N	c.1192_1193insAT	p.Ala398fs	1193/1260	398/419
01292020_IS	8063	21497	1.2%	1.8583E-54	X			+stop	High	N	c.1214A>G	p.Lys405*	1214/1260	405/419
01292020_IS	8114	17284	1.1%	7.311E-38	X			non coding	-	ORF10	c.-20A>G			
01292020_IS	8115	17309	10.7%	0E+00	X			non coding	-	ORF10	c.-19T>C			
01292020_IS	8120	16231	1.0%	1.3292E-33	X			non coding	-	ORF10	c.-14A>G			
01292020_IS	8122	16055	2.6%	5.6244E-104	X			non coding	-	ORF10	c.-12C>T			
02012020_NP	8124	19184	3.1%	7.3658E-153	X			non coding	-	ORF10	c.-10C>T			
02012020_NP	8150	14566	1.7%	8.8137E-58	X			ms	Moderate	ORF10	c.17T>C	p.Val6Ala	17/117	5/38
01292020_NP	8168	15091	1.5%	2.5633E-49	X			ms	Moderate	ORF10	c.35C>T	p.Thr12Met	35/117	11/38
01292020_IS	8236	4822	7.5%	1.0353E-104	X			ms	Moderate	ORF10	c.103T>C	p.Phe35Leu	103/117	35/38
02042020_NP	8238	5272	6.1%	6.9776E-90	X			syn	Low	ORF10	c.105T>C	p.Phe35Phe	105/117	35/38
01292020_IS	8253	4033	2.7%	6.3275E-28	X			non coding	-	S	c.*4293A>G			

Pos: position ; syn: synonymous mutation; ms: missense mutation; fs: frameshift ; +stop: apparition of STOP codon; -stop: disappearing of STOP codon; ORF: open reading frame ; Freq: frequency; Sub: substitution; Ins: insertion; Del: deletion; Prot. seq. Modif: protein sequence modification; CDS: coding DNA sequence; HGVS.c: sequence variant nomenclature, ".c" indicate that the type of reference sequence used is a coding DNA reference sequence; HGVS.p: sequence variant nomenclature, ".p" indicate that the type of reference sequence used is a protein reference sequence; S: spike; E: envelope; M: membrane; NC: nucleocapsid; NP: nasopharyngeal; IS: induced sputum. Variant identified in two different samples are highlighted in grey.

Supplementary Table 4: Characteristics of the 236 follow-up viral variant identified

Sample	POS	Depth	Frequency	Pvalue	Sub	Ins	Del	Prot seq. Modif	Impact on protein	Gene	HGVS.c	HGVS.p	CDS.pos / CDS.length	AA.pos / AA.length
02012020_NP	143	10153	17,3%	0	X			ms	Moderate	S	c.5T>C	p.Phe2Ser	5/3822	2/1273
02022020_NP	165	10873	9,2%	5,70E-290	X			syn	Low	S	c.27A>G	p.Pro9Pro	27/3822	9/1273
02012020_NP	172	13167	1,1%	5,70E-28	X			ms	Moderate	S	c.34T>C	p.Ser12Pro	34/3822	12/1273
01292020_NP	208	20697	12,1%	0	X			syn	Low	S	c.70T>C	p.Leu24Leu	70/3822	24/1273
01292020_IS	285	21791	5,2%	0	X			syn	Low	S	c.147T>C	p.His49His	147/3822	49/1273
01292020_NP	340	27193	1,5%	1,72E-90	X			ms	Moderate	S	c.202A>G	p.Met68Val	202/3822	68/1273
02022020_NP	580	14268	4,1%	1,70E-154	X			ms	Moderate	S	c.442A>G	p.Asn148Asp	442/3822	148/1273
02022020_NP	671	10285	5,4%	2,10E-153	X			ms	Moderate	S	c.533A>G	p.Asp178Gly	533/3822	178/1273
01292020_NP	745	8882	11,2%	2,96E-295	X			ms	Moderate	S	c.607A>G	p.Met203Val	607/3822	203/1273
02012020_NP	760	7903	1,8%	3,20E-33	X			ms	Moderate	S	c.622A>G	p.Thr208Ala	622/3822	208/1273
02042020_NP	781	14396	1,1%	1,06E-31	X			ms	Moderate	S	c.643G>A	p.Asp215Asn	643/3822	215/1273
02012020_NP	858	7755	1,5%	7,00E-28	X			syn	Low	S	c.720T>C	p.Thr240Thr	720/3822	240/1273
02012020_NP	947	8919	2,2%	5,00E-49	X			ms	Moderate	S	c.809T>C	p.Leu270Pro	809/3822	270/1273
02012020_NP	997	9628	99,8%	0	X			ms	Moderate	S	c.859G>A	p.Asp287Asn	859/3822	287/1273
01292020_IS	1041	18441	1,4%	2,46E-57	X			syn	Low	S	c.903T>C	p.Cys301Cys	903/3822	301/1273
02012020_NP	1111	16502	1,4%	7,00E-51	X			ms	Moderate	S	c.973T>C	p.Ser325Pro	973/3822	325/1273
02022020_NP	1146	17813	4,5%	2,20E-214	X			syn	Low	S	c.1008C>T	p.Cys336Cys	1008/3822	336/1273
02022020_NP	1166	17894	2,1%	2,10E-88	X			ms	Moderate	S	c.1028A>G	p.Asn343Ser	1028/3822	343/1273
01292020_NP	1254	19353	7,6%	0	X			syn	Low	S	c.1116A>G	p.Ala372Ala	1116/3822	372/1273
02012020_NP	1309	15950	1,2%	6,30E-39	X			ms	Moderate	S	c.1171T>C	p.Cys391Arg	1171/3822	391/1273
02012020_NP	1312	16038	1,8%	4,70E-67	X			ms	Moderate	S	c.1174T>C	p.Phe392Leu	1174/3822	392/1273
01292020_IS	1347	19015	1,1%	2,06E-42	X			syn	Low	S	c.1209A>G	p.Ter403Ter	1209/3822	403/1273
01292020_IS	1355	19013	1,6%	1,96E-69	X			ms	Moderate	S	c.1217A>G	p.Glu406Gly	1217/3822	406/1273
01292020_IS	1356	19074	1,6%	8,08E-66	X			syn	Low	S	c.1218A>G	p.Glu406Glu	1218/3822	406/1273

01292020_NP	1395	16647	1,4%	2,94E-52	X		syn	Low	S	c.1257T>C	p.Ala419Ala	1257/3822	419/1273
02012020_NP	1440	16364	2,0%	3,10E-75	X		syn	Low	S	c.1302A>G	p.Met434Met	1302/3822	434/1273
01292020_IS	1575	24299	2,1%	1,18E-119	X		syn	Low	S	c.1437T>C	p.Pro479Pro	1437/3822	479/1273
02022020_NP	1580	21350	1,3%	3,00E-61	X		ms	Moderate	S	c.1442A>G	p.Asn481Ser	1442/3822	481/1273
02012020_NP	1589	19557	2,0%	1,10E-89	X		ms	Moderate	S	c.1451A>G	p.Glu484Gly	1451/3822	484/1273
01292020_IS	1644	26537	1,1%	4,18E-61	X		syn	Low	S	c.1506T>C	p.Gly502Gly	1506/3822	502/1273
02022020_NP	1659	27912	2,4%	8,00E-167	X		syn	Low	S	c.1521A>G	p.Pro507Pro	1521/3822	507/1273
01292020_NP	1726	34596	1,2%	5,23E-83	X		ms	Moderate	S	c.1588T>C	p.Ser530Pro	1588/3822	530/1273
02022020_NP	1726	30839	2,4%	1,60E-181	X		ms	Moderate	S	c.1588T>C	p.Ser530Pro	1588/3822	530/1273
01292020_IS	1748	33208	4,4%	0	X		+stop	High	S	c.1610A>G	p.Lys537*	1610/3822	537/1273
02022020_NP	1758	31453	2,1%	1,00E-153	X		syn	Low	S	c.1620T>C	p.Asn540Asn	1620/3822	540/1273
02022020_NP	1883	36160	2,0%	1,40E-168	X		ms	Moderate	S	c.1745T>C	p.Leu582Pro	1745/3822	582/1273
01292020_NP	2008	40843	2,3%	2,42E-223	X		ms	Moderate	S	c.1870A>G	p.Ile624Val	1870/3822	624/1273
02012020_NP	2028	32384	1,4%	8,50E-101	X		syn	Low	S	c.1890T>C	p.Thr630Thr	1890/3822	630/1273
02022020_NP	2050	35251	1,1%	1,80E-74	X		ms	Moderate	S	c.1912A>G	p.Thr638Ala	1912/3822	638/1273
02012020_NP	2061	31733	1,3%	3,60E-90	X		syn	Low	S	c.1923T>C	p.Asn641Asn	1923/3822	641/1273
02012020_NP	2085	32069	1,1%	3,40E-70	X		syn	Low	S	c.1947T>C	p.Cys649Cys	1947/3822	649/1273
01292020_NP	2122	37192	1,3%	4,82E-98	X		ms	Moderate	S	c.1984T>C	p.Cys662Arg	1984/3822	662/1273
02022020_NP	2147	31047	1,4%	8,10E-92	X		ms	Moderate	S	c.2009T>C	p.Met670Thr	2009/3822	670/1273
01292020_NP	2216	32392	1,2%	6,74E-81	X		ms	Moderate	S	c.2078T>C	p.Ile693Thr	2078/3822	693/1273
02012020_NP	2223	27678	3,7%	2,10E-264	X		syn	Low	S	c.2085C>T	p.Tyr695Tyr	2085/3822	695/1273
01292020_IS	2376	28641	6,5%	0	X		syn	Low	S	c.2238A>G	p.Ser746Ser	2238/3822	746/1273
01292020_IS	2459	28789	1,2%	2,31E-72	X		ms	Moderate	S	c.2321A>G	p.Gln774Arg	2321/3822	774/1273
02012020_NP	2495	24039	1,7%	2,80E-90	X		+stop	High	S	c.2357A>G	p.Lys786*	2357/3822	786/1273
01292020_IS	2509	28643	1,0%	3,35E-58	X		ms	Moderate	S	c.2371A>G	p.Thr791Ala	2371/3822	791/1273
02012020_NP	2514	23630	2,5%	4,90E-142	X		syn	Low	S	c.2376A>G	p.Pro792Pro	2376/3822	792/1273
02022020_NP	2579	25373	8,8%	0,00E+00	X		+stop	High	S	c.2441A>G	p.Lys814*	2441/3822	814/1273
02012020_NP	2609	22108	1,1%	6,80E-50	X		ms	Moderate	S	c.2471A>G	p.Asn824Ser	2471/3822	824/1273

02022020_NP	2609	23895	2,5%	3,90E-150	X		ms	Moderate	S	c.2471A>G	p.Asn824Ser	2471/3822	824/1273
02012020_NP	2674	20229	1,4%	3,90E-62	X		ms	Moderate	S	c.2536G>A	p.Ala846Thr	2536/3822	846/1273
01292020_IS	2684	23647	10,4%	0	X		ms	Moderate	S	c.2546T>C	p.Leu849Pro	2546/3822	849/1273
02022020_NP	2688	20909	1,1%	7,10E-46	X		syn	Low	S	c.2550T>C	p.Ile850Ile	2550/3822	850/1273
01292020_IS	2714	22259	1,5%	3,09E-70	X		ms	Moderate	S	c.2576C>T	p.Thr859Ile	2576/3822	859/1273
01292020_IS	2776	21710	2,4%	3,56E-128	X		ms	Moderate	S	c.2638G>A	p.Gly880Ser	2638/3822	880/1273
01292020_NP	2805	22965	1,6%	1,80E-80	X		syn	Low	S	c.2667T>C	p.Gly889Gly	2667/3822	889/1273
01292020_NP	2868	26300	4,2%	1,97E-290	X		syn	Low	S	c.2730A>G	p.Gly910Gly	2730/3822	910/1273
02022020_NP	2959	25791	1,4%	6,80E-80	X		ms	Moderate	S	c.2821A>G	p.Thr941Ala	2821/3822	941/1273
02012020_NP	2993	22793	1,1%	1,10E-50	X		ms	Moderate	S	c.2855T>C	p.Val952Ala	2855/3822	952/1273
02012020_NP	3028	24010	3,6%	1,20E-222	X		ms	Moderate	S	c.2890A>G	p.Lys964Glu	2890/3822	964/1273
01292020_NP	3030	30260	1,2%	1,59E-71	X		syn	Low	S	c.2892A>G	p.Lys964Lys	2892/3822	964/1273
02022020_NP	3030	27014	2,6%	7,50E-176	X		syn	Low	S	c.2892A>G	p.Lys964Lys	2892/3822	964/1273
01312020_NP	3061	34219	1,9%	3,54E-145	X		ms	Moderate	S	c.2923A>G	p.Ser975Gly	2923/3822	975/1273
02022020_NP	3084	27242	3,8%	2,50E-268	X		syn	Low	S	c.2946A>G	p.Ser982Ser	2946/3822	982/1273
01292020_NP	3101	30083	1,3%	3,50E-80	X		ms	Moderate	S	c.2963A>T	p.Glu988Val	2963/3822	988/1273
01312020_NP	3142	32963	95,9%	0		X	fs	High	S	c.3007delA	p.Ser1003fs	3007/3822	1003/1273
02022020_NP	3151	26391	8,5%	0,00E+00	X		+stop	High	S	c.3013C>T	p.Gln1005*	3013/3822	1005/1273
01292020_NP	3284	29684	1,0%	7,27E-61	X		ms	Moderate	S	c.3146T>C	p.Leu1049Pro	3146/3822	1049/1273
02022020_NP	3318	27872	11,3%	0,00E+00	X		syn	Low	S	c.3180A>G	p.Val1060Val	3180/3822	1060/1273
02022020_NP	3320	28389	3,7%	1,80E-270	X		ms	Moderate	S	c.3182T>G	p.Val1061Gly	3182/3822	1061/1273
02012020_NP	3404	24030	1,6%	1,20E-86	X		ms	Moderate	S	c.3266T>C	p.Phe1089Ser	3266/3822	1089/1273
02012020_NP	3405	23991	1,6%	5,40E-89	X		syn	Low	S	c.3267T>C	p.Phe1089Phe	3267/3822	1089/1273
02012020_NP	3419	23857	3,6%	3,80E-225	X		ms	Moderate	S	c.3281T>C	p.Val1094Ala	3281/3822	1094/1273
01292020_IS	3421	28286	1,1%	8,60E-60	X		ms	Moderate	S	c.3283T>G	p.Phe1095Val	3283/3822	1095/1273
02022020_NP	3431	26850	6,3%	0,00E+00	X		ms	Moderate	S	c.3293A>G	p.Asn1098Ser	3293/3822	1098/1273
01292020_IS	3450	29153	1,0%	1,70E-58	X		syn	Low	S	c.3312A>G	p.Val1104Val	3312/3822	1104/1273
01292020_NP	3479	31053	2,5%	1,77E-186	X		ms	Moderate	S	c.3341T>C	p.Ile1114Thr	3341/3822	1114/1273

01292020_NP	3614	30845	21,7%	0	X		ms	Moderate	S	c.3476A>G	p.His1159Arg	3476/3822	1159/1273
01312020_NP	3636	29593	1,9%	7,36E-127	X		syn	Low	S	c.3498A>G	p.Leu1166Leu	3498/3822	1166/1273
01292020_NP	3641	28685	1,2%	1,78E-70	X		ms	Moderate	S	c.3503A>G	p.Asp1168Gly	3503/3822	1168/1273
01312020_NP	3692	28799	99,9%	0	X		ms	Moderate	S	c.3554G>T	p.Arg1185Leu	3554/3822	1185/1273
01292020_IS	3700	28435	1,0%	1,82E-58	X		ms	Moderate	S	c.3562G>A	p.Glu1188Lys	3562/3822	1188/1273
02022020_NP	3723	24864	2,2%	2,40E-129	X		syn	Low	S	c.3585A>G	p.Glu1195Glu	3585/3822	1195/1273
02012020_NP	3853	18580	8,0%	0	X		ms	Moderate	S	c.3715A>G	p.Ser1239Gly	3715/3822	1239/1273
02022020_NP	3883	19176	1,1%	5,00E-40	X		ms	Moderate	S	c.3745T>C	p.Ser1249Pro	3745/3822	1249/1273
02012020_NP	3914	16759	1,7%	2,20E-63	X		ms	Moderate	S	c.3776A>G	p.Asp1259Gly	3776/3822	1259/1273
01292020_NP	3939	19040	4,6%	5,32E-234	X		syn	Low	S	c.3801A>G	p.Gly1267Gly	3801/3822	1267/1273
01292020_NP	3978	17011	1,0%	1,22E-33	X		ms	Moderate	ORF3a	c.10T>C	p.Phe4Leu	10/828	4/275
01292020_NP	3986	16202	1,3%	5,86E-46	X		syn	Low	ORF3a	c.18A>G	p.Ter6Ter	18/828	6/275
02012020_NP	4018	11400	1,2%	1,80E-28	X		ms	Moderate	ORF3a	c.50A>G	p.Gln17Arg	50/828	17/275
02022020_NP	4034	11803	2,2%	8,60E-64	X		syn	Low	ORF3a	c.66T>C	p.Asp22Asp	66/828	22/275
02022020_NP	4155	6265	4,2%	2,90E-70	X		ms	Moderate	ORF3a	c.187A>G	p.Met63Val	187/828	63/275
02022020_NP	4203	11874	1,1%	2,10E-27	X		ms	Moderate	ORF3a	c.235T>C	p.Phe79Leu	235/828	79/275
02022020_NP	4219	13091	4,6%	2,20E-162	X		ms	Moderate	ORF3a	c.251T>C	p.Leu84Pro	251/828	84/275
02042020_NP	4220	8907	2,0%	5,38E-43		X	fs	High	ORF3a	c.255_283delGTTGTTTGTAACAGTTTACTCACACCTTT	p.Leu85fs	255/828	85/275
01292020_NP	4251	13136	1,0%	6,53E-27	X		syn	Low	ORF3a	c.283T>C	p.Leu95Leu	283/828	95/275
02012020_NP	4256	12286	12,3%	0	X		syn	Low	ORF3a	c.288C>T	p.Leu96Leu	288/828	96/275
01292020_NP	4270	14064	1,7%	5,45E-55	X		ms	Moderate	ORF3a	c.302T>C	p.Leu101Pro	302/828	101/275
02012020_NP	4295	14803	3,1%	1,50E-117	X		syn	Low	ORF3a	c.327T>C	p.Tyr109Tyr	327/828	109/275
02022020_NP	4298	20657	1,4%	8,80E-64	X		syn	Low	ORF3a	c.330T>C	p.Ala110Ala	330/828	110/275
02012020_NP	4374	20962	2,2%	2,80E-108	X		ms	Moderate	ORF3a	c.406A>G	p.Lys136Glu	406/828	136/275
01292020_IS	4391	17332	1,6%	2,62E-61	X		syn	Low	ORF3a	c.423T>C	p.Tyr141Tyr	423/828	141/275
02032020_NP	4402	27230	2,6%	4,04E-174		X	fs	High	ORF3a	c.435_438delTTTT	p.Leu147fs	435/828	145/275
02012020_NP	4417	22555	1,5%	7,00E-72	X		ms	Moderate	ORF3a	c.449A>G	p.His150Arg	449/828	150/275
01312020_NP	4443	28821	2,6%	2,33E-185	X		ms	Moderate	ORF3a	c.475C>T	p.Pro159Ser	475/828	159/275

01292020_NP	4513	30487	1,9%	1,90E-135	X		ms	Moderate	ORF3a	c.545A>G	p.His182Arg	545/828	182/275
01292020_IS	4551	22658	1,8%	9,31E-97	X		ms	Moderate	ORF3a	c.583T>C	p.Ser195Pro	583/828	195/275
02022020_NP	4556	39633	1,0%	3,30E-77	X		syn	Low	ORF3a	c.588A>G	p.Gly196Gly	588/828	196/275
02012020_NP	4588	31322	1,0%	1,70E-62	X		ms	Moderate	ORF3a	c.620T>C	p.Phe207Ser	620/828	207/275
02012020_NP	4621	32898	1,4%	5,50E-103	X		ms	Moderate	ORF3a	c.653A>G	p.Gln218Arg	653/828	218/275
02042020_NP	4629	31880	1,5%	2,70E-105	X		ms	Moderate	ORF3a	c.661A>G	p.Thr221Ala	661/828	221/275
02022020_NP	4688	45488	1,1%	2,10E-97	X		syn	Low	ORF3a	c.720T>C	p.Pro240Pro	720/828	240/275
01292020_NP	4832	30787	1,2%	4,35E-76	X		syn	Low	E	c.12C>T	p.Phe4Phe	12/228	4/75
02012020_NP	4841	27872	1,3%	4,10E-75	X		syn	Low	E	c.21A>G	p.Glu7Glu	21/228	7/75
02022020_NP	4871	32976	3,2%	2,30E-271	X		syn	Low	E	c.51A>G	p.Val17Val	51/228	17/75
01312020_NP	4875	30850	2,5%	2,25E-191			fs	High	E	c.60dupT	p.Leu21fs	61/228	21/75
01312020_NP	4881	30018	4,0%	0	X		ms	Moderate	E	c.61C>T	p.Leu21Phe	61/228	21/75
01292020_NP	4979	24878	2,1%	4,68E-121	X		syn	Low	E	c.159A>G	p.Lys53Lys	159/228	53/75
02022020_NP	5014	22934	1,1%	1,50E-52	X		ms	Moderate	E	c.194T>C	p.Leu65Pro	194/228	65/75
01292020_NP	5029	24454	1,1%	1,07E-54	X		ms	Moderate	E	c.209T>C	p.Val70Ala	209/228	70/75
02012020_NP	5071	14178	5,6%	8,40E-218	X		non coding	-	M	c.-28T>C			
01292020_NP	5084	22783	1,8%	8,38E-93	X		non coding	-	M	c.-15A>G			
02032020_NP	5087	17014	1,4%	9,89E-50	X		non coding	-	M	c.-12T>C			
01292020_IS	5092	15779	8,6%	0	X		non coding	-	M	c.-7T>C			
01292020_NP	5099	22852	1,2%	1,37E-56	X		start lost	High	M	c.1A>C	p.Met1?	1/669	1/222
02022020_NP	5104	18922	1,7%	1,70E-71	X		syn	Low	M	c.6A>G	p.Ala2Ala	6/669	2/222
02022020_NP	5149	20579	1,7%	1,90E-82	X		syn	Low	M	c.51T>C	p.Leu17Leu	51/669	17/222
02012020_NP	5173	15735	1,1%	5,70E-36	X		syn	Low	M	c.75T>C	p.Gly25Gly	75/669	25/222
01292020_IS	5175	16726	1,1%	3,01E-36	X		ms	Moderate	M	c.77T>C	p.Phe26Ser	77/669	26/222
01292020_NP	5304	26859	3,0%	1,85E-207	X		ms	Moderate	M	c.206C>T	p.Ala69Val	206/669	69/222
02022020_NP	5308	30125	2,7%	1,80E-202	X		syn	Low	M	c.210T>C	p.Val70Val	210/669	70/222
02012020_NP	5379	25273	1,6%	1,50E-91	X		ms	Moderate	M	c.281G>A	p.Ser94Asn	281/669	94/222
01292020_IS	5444	22587	1,1%	3,20E-51	X		ms	Moderate	M	c.346A>G	p.Thr116Ala	346/669	116/222

02012020_NP	5465	28156	48,2%	0	X		ms	Moderate	M	c.367C>T	p.Pro123Ser	367/669	123/222
01292020_NP	5467	29260	2,3%	7,76E-165	X		syn	Low	M	c.369A>C	p.Pro123Pro	369/669	123/222
01292020_IS	5511	23455	3,0%	9,93E-177	X		ms	Moderate	M	c.413T>C	p.Leu138Pro	413/669	138/222
02022020_NP	5512	37912	46,7%	0,00E+00	X		syn	Low	M	c.414C>T	p.Leu138Leu	414/669	138/222
01292020_IS	5559	23687	1,1%	9,31E-52	X		ms	Moderate	M	c.461A>G	p.His154Arg	461/669	154/222
02012020_NP	5566	29888	3,5%	4,70E-271	X		syn	Low	M	c.468A>G	p.Leu156Leu	468/669	156/222
02022020_NP	5620	34716	1,3%	5,10E-90	X		syn	Low	M	c.522A>G	p.Arg174Arg	522/669	174/222
02042020_NP	5664	23869	8,0%	0,00E+00	X		ms	Moderate	M	c.566G>A	p.Gly189Asp	566/669	189/222
02022020_NP	5680	31895	1,7%	2,00E-123	X		syn	Low	M	c.582T>C	p.Ala194Ala	582/669	194/222
01292020_IS	5691	20823	11,8%	0	X		ms	Moderate	M	c.593G>A	p.Arg198His	593/669	198/222
01292020_NP	5727	24055	3,4%	1,28E-209	X		ms	Moderate	M	c.629A>G	p.His210Arg	629/669	210/222
01292020_IS	5748	17579	1,4%	1,47E-53	X		ms	Moderate	M	c.650T>C	p.Ile217Thr	650/669	217/222
01292020_IS	5753	17221	2,9%	2,99E-127	X		syn	Low	M	c.655T>C	p.Leu219Leu	655/669	219/222
01292020_IS	5758	17186	2,9%	1,89E-123	X		syn	Low	M	c.660T>C	p.Leu220Leu	660/669	220/222
01292020_IS	5773	15670	9,3%	0	X		non coding	-	ORF6	c.-5A>G			
01292020_IS	5797	14988	18,7%	0	X		ms	Moderate	ORF6	c.20T>A	p.Phe7Tyr	20/186	7/61
01292020_IS	5815	11765	1,3%	1,23E-33	X		ms	Moderate	ORF6	c.38A>G	p.Glu13Gly	38/186	13/61
01312020_NP	5821	17614	3,7%	2,50E-173	X		ms	Moderate	ORF6	c.44T>C	p.Leu15Ser	44/186	15/61
02032020_NP	5937	10555	1,3%	1,38E-29	X		ms	Moderate	ORF6	c.160G>A	p.Glu54Lys	160/186	54/61
02022020_NP	5939	8469	1,4%	7,40E-26	X		syn	Low	ORF6	c.162A>G	p.Glu54Glu	162/186	54/61
02032020_NP	5961	11849	1,8%	1,14E-48		X	fs	High	ORF6	c.184_185insTCTCC	p.Ter62fs	185/186	62/61
02022020_NP	5988	8378	2,1%	7,10E-42	X		ms	Moderate	ORF7a	c.19T>A	p.Leu7Met	19/366	7/121
02012020_NP	5990	11840	1,4%	3,30E-37	X		syn	Low	ORF7a	c.21G>A	p.Leu7Leu	21/366	7/121
02022020_NP	5990	8696	5,8%	1,40E-141		X	fs	High	ORF7a	c.21_22insA	p.Ala8fs	22/366	8/121
01292020_IS	5999	12072	1,3%	1,33E-33	X		syn	Low	ORF7a	c.30A>G	p.Met10Met	30/366	10/121
01292020_IS	6077	14467	1,1%	3,12E-32	X		syn	Low	ORF7a	c.108T>C	p.Ser36Ser	108/366	36/121
01292020_IS	6119	15505	1,3%	1,22E-41	X		syn	Low	ORF7a	c.150T>C	p.Ala50Ala	150/366	50/121
02022020_NP	6166	15235	1,0%	5,50E-32	X		ms	Moderate	ORF7a	c.197C>T	p.Ala66Val	197/366	66/121

01292020_NP	6207	16759	1,3%	2,08E-48	X		-stop	High	ORF7a	c.238A>G	p.Ter80Glyext*?	238/366	80/121
02012020_NP	6238	25320	1,5%	5,50E-86	X		ms	Moderate	ORF7a	c.269A>G	p.Gln90Arg	269/366	90/121
01292020_NP	6312	12311	1,1%	1,12E-27	X		ms	Moderate	ORF7a	c.343A>G	p.Thr115Ala	343/366	115/121
01292020_NP	6361	10377	12,4%	0		X	fs	High	ORF7b	c.31_32insCAAACAT	p.Leu11fs	32/132	11/43
01292020_NP	6364	9620	15,6%	0		X	Conservative inframe	Moderate	ORF7b	c.33_34insGCCGCAAAT	p.Leu11_Cys12insAlaAlaAsn	34/132	12/43
02032020_NP	6373	19491	2,7%	1,48E-128	X		syn	Low	ORF7b	c.42A>G	p.Leu14Leu	42/132	14/43
02032020_NP	6376	19374	1,4%	4,06E-61		X	fs	High	ORF7b	c.45_46insGCAAATTGCACAA	p.Phe16fs	46/132	16/43
01292020_IS	6387	20212	18,2%	0	X		ms	Moderate	ORF7b	c.56T>C	p.Phe19Ser	56/132	19/43
02022020_NP	6541	16595	1,5%	1,20E-53	X		syn	Low	ORF8	c.72A>G	p.Ser24Ser	72/366	24/121
02032020_NP	6543	16338	1,5%	1,54E-52	X		ms	Moderate	ORF8	c.74G>T	p.Cys25Phe	74/366	25/121
01292020_IS	6622	16391	3,5%	1,42E-151	X		syn	Low	ORF8	c.153T>C	p.Ala51Ala	153/366	51/121
01292020_IS	6743	17832	1,3%	1,54E-50	X		ms	Moderate	ORF8	c.274G>A	p.Glu92Lys	274/366	92/121
01292020_NP	6791	8376	16,4%	0	X		ms	Moderate	ORF8	c.322T>C	p.Phe108Leu	322/366	108/121
02022020_NP	6850	19211	4,9%	1,50E-257	X		Initiator codon variant	Low	N	c.1A>G	p.Met1?	1/1260	1/419
02012020_NP	6914	26671	1,8%	8,60E-107	X		ms	Moderate	N	c.65A>G	p.Asp22Gly	65/1260	22/419
02022020_NP	6934	19286	4,2%	3,40E-213	X		ms	Moderate	N	c.85A>G	p.Asn29Asp	85/1260	29/419
01292020_IS	6975	18251	1,2%	3,32E-43	X		syn	Low	N	c.126C>T	p.Pro42Pro	126/1260	42/419
02022020_NP	6984	18556	1,1%	1,60E-40	X		syn	Low	N	c.135A>G	p.Leu45Leu	135/1260	45/419
02022020_NP	7050	18173	1,3%	7,30E-52	X		syn	Low	N	c.201T>C	p.Pro67Pro	201/1260	67/419
02022020_NP	7052	18200	3,4%	1,40E-161	X		ms	Moderate	N	c.203G>A	p.Arg68Gln	203/1260	68/419
01292020_IS	7059	17703	16,8%	0	X		syn	Low	N	c.210A>G	p.Gln70Gln	210/1260	70/419
02012020_NP	7099	24182	2,8%	2,70E-167	X		ms	Moderate	N	c.250A>G	p.Ile84Val	250/1260	84/419
02022020_NP	7116	17704	3,1%	6,80E-142	X		syn	Low	N	c.267A>G	p.Ter89Ter	267/1260	89/419
02032020_NP	7116	16921	1,3%	1,39E-47	X		syn	Low	N	c.267A>G	p.Ter89Ter	267/1260	89/419
02012020_NP	7164	24413	1,9%	1,90E-105	X		syn	Low	N	c.315T>C	p.Ser105Ser	315/1260	105/419
02042020_NP	7179	25326	10,5%	0,00E+00	X		syn	Low	N	c.330C>T	p.Phe110Phe	330/1260	110/419
01292020_IS	7259	16469	12,5%	0	X		ms	Moderate	N	c.410G>A	p.Gly137Glu	410/1260	137/419
02022020_NP	7260	16636	1,1%	1,90E-39	X		syn	Low	N	c.411A>G	p.Gly137Gly	411/1260	137/419

02022020_NP	7282	16758	10,7%	0,00E+00	X			ms	Moderate	N	c.433C>T	p.His145Tyr	433/1260	145/419
01292020_IS	7283	15853	2,7%	8,95E-108	X			ms	Moderate	N	c.434A>G	p.His145Arg	434/1260	145/419
01292020_IS	7342	15999	3,2%	1,29E-133	X			ms	Moderate	N	c.493A>G	p.Thr165Ala	493/1260	165/419
02012020_NP	7410	23241	2,7%	4,40E-153	X			syn	Low	N	c.561A>G	p.Ser187Ser	561/1260	187/419
01292020_IS	7411	15973	1,5%	1,64E-51	X			ms	Moderate	N	c.562T>C	p.Ser188Pro	562/1260	188/419
02022020_NP	7416	16062	6,4%	3,80E-288	X			syn	Low	N	c.567T>C	p.Arg189Arg	567/1260	189/419
02022020_NP	7464	15493	2,3%	1,80E-85	X			syn	Low	N	c.615T>C	p.Thr205Thr	615/1260	205/419
02022020_NP	7470	15401	1,1%	3,00E-36	X			syn	Low	N	c.621T>C	p.Pro207Pro	621/1260	207/419
01312020_NP	7499	26214	4,1%	9,36E-282	X			ms	Moderate	N	c.650C>T	p.Ala217Val	650/1260	217/419
01292020_IS	7509	14683	2,2%	2,11E-79	X			syn	Low	N	c.660T>C	p.Ala220Ala	660/1260	220/419
01292020_IS	7567	13890	2,3%	8,43E-79	X			+stop	High	N	c.718C>T	p.Gln240*	718/1260	240/419
02032020_NP	7599	10602	1,9%	1,00E-47	X			syn	Low	N	c.750T>C	p.Ser250Ser	750/1260	250/419
01292020_IS	7615	14022	1,9%	9,50E-63	X			ms	Moderate	N	c.766A>C	p.Lys256Gln	766/1260	256/419
01292020_IS	7616	13996	1,3%	1,88E-38	X			+stop	High	N	c.767A>G	p.Lys256*	767/1260	256/419
02022020_NP	7638	12989	2,3%	6,90E-74	X			syn	Low	N	c.789T>C	p.Thr263Thr	789/1260	263/419
01292020_IS	7668	12915	1,9%	7,94E-60	X			syn	Low	N	c.819T>C	p.Ala273Ala	819/1260	273/419
01292020_IS	7698	13047	1,0%	1,19E-26	X			syn	Low	N	c.849A>G	p.Gln283Gln	849/1260	283/419
01292020_NP	7729	6034	2,2%	2,57E-32		X		Disruptive inframe	Moderate	N	c.881_882insGAATGA	p.Gln294_Gly295insAsnGlu	882/1260	294/419
01292020_IS	7731	14110	1,6%	4,43E-51		X		Conservative inframe	Moderate	N	c.882_883insATT	p.Gln294_Gly295insIle	883/1260	295/419
01292020_NP	7736	7613	20,8%	0		X		fs	High	N	c.888_889insTT	p.Asp297fs	889/1260	297/419
01292020_IS	7739	14577	2,8%	3,71E-101		X		Disruptive inframe	Moderate	N	c.890_891insCTTGCT	p.Asp297_Tyr298insLeuLeu	891/1260	297/419
02032020_NP	7739	11045	1,4%	3,43E-36		X		fs	High	N	c.890_891insCTTCTATT TGTGCTTT	p.Tyr298fs	891/1260	297/419
01292020_NP	7741	6212	3,6%	3,24E-59			X	fs	High	N	c.893delA	p.Tyr298fs	893/1260	298/419
02032020_NP	7741	11064	2,4%	7,86E-64		X		fs	High	N	c.892_893insGA	p.Tyr298fs	893/1260	298/419
01292020_IS	7742	14676	2,6%	2,79E-93		X		fs	High	N	c.893_894insG	p.Tyr298fs	894/1260	298/419
02042020_NP	7743	22632	11,9%	0,00E+00	X			syn	Low	N	c.894C>T	p.Tyr298Tyr	894/1260	298/419
02012020_NP	7746	20442	1,1%	2,80E-44	X			syn	Low	N	c.897A>G	p.Lys299Lys	897/1260	299/419
02032020_NP	7776	12993	3,5%	2,87E-120	X			syn	Low	N	c.927C>T	p.Pro309Pro	927/1260	309/419

02012020_NP	7799	21842	1,2%	6,50E-54	X		ms	Moderate	N	c.950T>C	p.Met317Thr	950/1260	317/419
02032020_NP	7829	16721	1,6%	2,02E-61	X		ms	Moderate	N	c.980C>T	p.Ser327Leu	980/1260	327/419
02032020_NP	7833	16714	1,7%	4,97E-67	X		syn	Low	N	c.984A>G	p.Gly328Gly	984/1260	328/419
01312020_NP	7868	31788	1,5%	2,69E-105	X		ms	Moderate	N	c.1019A>G	p.Asp340Gly	1019/1260	340/419
02022020_NP	8041	17844	1,4%	7,90E-54		X	fs	High	N	c.1192_1193insAT	p.Ala398fs	1193/1260	398/419
01292020_IS	8063	21497	1,2%	1,86E-54	X		+stop	High	N	c.1214A>G	p.Lys405*	1214/1260	405/419
01292020_IS	8114	17284	1,1%	7,31E-38	X		non coding	-	ORF10	c.-20A>G			
01292020_IS	8115	17309	10,7%	0	X		non coding	-	ORF10	c.-19T>C			
01292020_IS	8120	16231	1,0%	1,33E-33	X		non coding	-	ORF10	c.-14A>G			
01292020_IS	8122	16055	2,6%	5,62E-104	X		non coding	-	ORF10	c.-12C>T			
02012020_NP	8124	19194	3,1%	7,40E-153	X		non coding	-	ORF10	c.-10C>T			
02012020_NP	8150	14566	1,7%	8,80E-58	X		ms	Moderate	ORF10	c.17T>C	p.Val6Ala	17/117	6/38
01292020_NP	8168	15091	1,5%	2,56E-49	X		ms	Moderate	ORF10	c.35C>T	p.Thr12Met	35/117	12/38
01292020_IS	8236	4822	7,5%	1,04E-104	X		ms	Moderate	ORF10	c.103T>C	p.Phe35Leu	103/117	35/38
02042020_NP	8238	5272	6,1%	6,98E-90	X		syn	Low	ORF10	c.105T>C	p.Phe35Phe	105/117	35/38
01292020_IS	8253	4033	2,7%	6,33E-28	X		non coding	-	S	c.*4293A>G			

Pos: position ; syn: synonymous mutation; ms: missense mutation; fs: frameshift ; +stop: apparition of STOP codon; -stop: disappearing of STOP codon; ORF: open reading frame ; Freq: frequency; Sub: substitution; Ins: insertion; Del: deletion; Prot. seq. Modif: protein sequence modification; CDS: coding DNA sequence; HGVS.c: sequence variant nomenclature, ".c" indicate that the type of reference sequence used is a coding DNA reference sequence; HGVS.p: sequence variant nomenclature, ".p" indicate that the type of reference sequence used is a protein reference sequence; S: spike; E: envelope; M: membrane; NC: nucleocapsid; NP: nasopharyngeal; IS: induced sputum.

Variant identified in two different samples are highlighted in grey.

Variant identified only during follow-up (compared to intra-sample variant) are highlighted in red.